NUREG/CR-1569
R6, RA

Seismicity and Tectonic Relationships for Upper Great Lakes Precambrian Shield Province

Final Report

Manuscript Completed: June 1980
Date Published: July 1980

Prepared by
H. M. Mooney, M. Walton*

Department of Geology and Geophysics
University of Minnesota
Minneapolis, MN 55455

*Minnesota Geological Survey
1633 Eustis Street
St. Paul, MN 55108

Prepared for
Division of Reactor Safety Research
Office of Nuclear Regulatory Research
U.S. Nuclear Regulatory Commission
Washington, D.C. 20555
NRC FIN No. B5952
Under Contract No. NRC-04-76-289

ABSTRACT

This is a final report comprising a three year study of the seismicity of Minnesota including the procurement and installation of a six station seismograph system. This system was deployed in a microearthquake monitoring array. An earth model was developed based on signals from mine blasts and regular earthquake bulletins were published. Descriptions of the model, methodologies, and three significant earthquakes are given.

TABLE OF CONTENTS

LIST OF FIGURES

LIST OF FIGURES (Continued)

LIST OF TABLES

I. Extended Summary; Background and Purpose

The Central Minnesota Seismic Array (CMSA) started operation on 1 January, 1977. The goal was to establish a seismicity data base for the Upper Great Lakes Precambrian Shield Province. The location of the array placed particular emphasis on known seismicity along the Morris Fault in central Minnesota, a major element of the Great Lakes Tectonic Zone (Sims, P.K., and others, in press; Mooney, 1979; Mooney and Morey, 1980), and on possible seismicity along a major tectonic element of North America known as the Midcontinent Gravity High (Mooney, et al., 1970a; 1970b).

The CMSA consists of six 1-second seismometers placed along the circumference and at the center of a circle of diameter 27 km. To avoid cultural noise, the array was located in a rural area of central Minnesota near Mora, with data telemetered 100 km by phone line to Minneapolis. The array location was also chosen with consideration of the two features mentioned above. First, we have established (Greenhalgh, 1979) that array detection capability along the full length of the Morris Fault extends down to about magnitude 2. Second, the array was placed slightly west of the western boundary fault (the Douglas Fault) of the Midcontinent Gravity High, in a region where upper crustal structure has been well determined by a number of seismic refraction profiles (Mooney et al., ibid).

The primary functions of the array are detection, location, and parameterization of local and regional events. Three such events have been recorded to date, as discussed below. A great deal of preliminary and ongoing effort has also been involved, however, which has been documented in approximately 35 reports to USNRC, theses, and publications, as well as oral presentations at meetings. This effort may be described under four headings.

1) Routine array operation.

The six seismometer outputs are transmitted via telephone line about 100 km to Minneapolis where they are recorded on a 7-channel 5-day magnetic tape recorder. One channel is also monitored on a Sprengnether visual recorder. Full information on the array is provided in Technical Report 1978-4, System Documentation for Central Minnesota Seismic Array and Affiliated Stations.

The recorded events include teleseisms from around the world, mine blasts from the Mesabi Iron Range (200 km) and others up to 300 km, and a few local earthquakes. Cultural and wind noise affecting any one seismometer can be easily recognized because playbacks from all stations are displayed side by side on a common time base, including WWVB time code.

The data analysis starts with a search for events which correlate on two or more of the seismometers. This search is carried out jointly on the Sprengnether record and on a compressed playback of the six array stations.

Each identified event is played back from the magnetic tape at much higher speed, normally 4"/second and occasionally 8"/second. These playbacks form the basic data set for the CMSA. They occupy several hundred boxes in a data repository at the University of Minnesota. Every event has been studied and catalogued. Certain events of particular interest have been more thoroughly studied. Some have been digitized and stored in the University computer system.

Routine array operation involves also a certain amount of equipment maintenance. We have had some troubles with both the Geotech 5-day tape recorder and the Honeywell playback tape recorder. The former resulted in down time on the system. The latter did not because we could postpone the playbacks. The Geotech electronic components (amplifiers, VCOs, demodulators) have proved quite reliable, but on several occasions lightning strikes have caused damage, in one case so severe that we had to purchase a replacement unit. These occasions resulted in array operation with less than six full channels. The Geotech seismometers have operated reliably; our lightning protection system seems to have worked for them.

The final outputs from routine array operation are the Seismic Event Logs. These have been issued on a quarterly basis. As noted later, we feel that these Event Logs have now served their purpose and should be replaced by another type of report in any further operation of CMSA.

2) System calibration

A great deal of effort has gone into calibration of the CMSA with respect to event location and magnitude calibration. This effort is documented in many of the technical reports and theses. We feel that the effort has paid off and that the array may now be considered as well calibrated.

One calibration effort was directed toward a study of array bias. The goal was to compare known against observed direction and apparent horizontal slowness. Teleseismic events were used. The outcome of the analysis was a table of station corrections for each of the six array stations. By applying these corrections to the raw arrival times, the azimuth and distance computations from the array have been significantly improved. The analysis was actually carried out twice (Technical Reports 1978-1 and 1979-1), the second time on a much larger data base of events, although as it turned out the station corrections were not significantly altered.

An interesting sidelight of the array bias study was that it confirmed the upper crustal structure obtained previously from the seismic refraction profiles (Mooney et al., 1970a; 1970b). Stating it another way, the station corrections could be accounted for from known geologic structure. A corollary would be that deep crustal/upper mantle geologic variations are not significant over the dimensions of the array.

The array bias investigation included also a similar study for Mesabi mine blasts. The results are given in the two Technical Reports cited above.

The second aspect of array calibration was directed toward magnitude determination. Two bountiful sources of data were available: teleseisms and mine blasts from the Mesabi Iron Range. Teleseismic magnitudes are conveniently available from the National Earthquake Information Service. For the mine blasts, we were able to obtain explosive weights through the generous cooperation of the seven mining companies. The methods to convert these to magnitude equivalents are described in theses by S.A. Greenhalgh (1979) and C.C. Mosher (1979).

3) Regional geologic studies

These form part of the array calibration, but we will describe them separately. The goal is to maximize information about seismic velocity distribution in the region under study, since event location depends strongly upon the velocity model used.

The first study is presented in a thesis by R.A. Anderson (1978). A brief summary appears as Technical Report 1978-3. The study produced a long range seismic refraction profile extending from CMSA for 160 km north, to a mine blast source near Keewatin Minnesota. The preliminary interpretation yielded a rough crustal/upper mantle velocity model for the region to the north of the array. The data were too sparse to be definitive, however. One striking result was the suggestion of a major tectonic boundary trending east-west, about 100 km north of CMSA. This lies on a projection of the earthquake epicenter trend associated with the Morris Fault in central Minnesota (Mooney, 1979; Mooney and Morey, 1980). The delineation of this boundary thus has significance in assessing regional seismicity.

The work by Anderson showed the importance of the refraction profile to the goals of the CMSA program. For this reason, a new program has been set up to obtain similar measurements but with higher precision and closer station spacing. The program is being conducted by N.A. Wattrus. He uses larger blasts, from the U.S. Steel mine at Mountain Iron, Minnesota. He proposes to obtain a basic suite of data at 10 km intervals for 180 km south to the CMSA location, with additional data points filled in if required. The ever-difficult problem of determining zero or blast time has been approached by placing a permanent seismometer near the mine site, with telemetering via telephone to a recording system in Minneapolis. The program proceeds slowly because blasts occur only once a week or so.

The second geologic study, recently completed by C.C. Mosher (1980) deals with Rayleigh waves produced by Mesabi mine blasts. The pattern of these surface waves differs from mine to mine, and from CMSA station to station. Frequently there are two distinct arrivals coming from different azimuths for the same mine blast.

Surface wave analysis yields a different kind of geologic information than does seismic body wave analysis. Surface waves provide a weighted average for the velocity distribution in the uppermost few kilometers of the earth (for the period range observed here). Furthermore, surface waves are especially sensitive to shear wave velocities.

Our early analysis of the observed surface waves attributed the geologic significance to the total 200-km path from the Mesabi Iron Range to the CMSA location. Since geology varies significantly along the path, the interpretation would thus represent some sort of weighted average, resulting in considerable ambiguity. We assumed that the two distinct surface wave arrivals represented two Rayleigh wave modes.

More careful analysis, however, revealed that we are observing something entirely different from the above. The following characteristics of the observed surface wave patterns led us to this conclusion:

1. The apparent horizontal velocities across the array are too low to represent an average value over a 5-20 km depth interval.
2. The apparent horizontal velocities for the two surface wave arrivals are markedly different.
3. The surface waves arrive only a few seconds after the S wave group. This would be impossible if the surface waves had travelled all the way from the source at the measured apparent horizontal velocity.
4. The azimuth (direction of arrival) of the two surface waves groups differ from known direction to the source and differ also from each other.
5. The energy in both surface wave arrivals falls in essentially the same frequency band (0.5-2 seconds period), which would not be expected if we are observing two Rayleigh wave modes.
6. The seismic wave forms for the surface waves differ substantially in moving from one array station to the next.

These observations lead us to conclude that the surface waves are being regenerated in the general vicinity of CMSA, and that the two arrivals represent multipathing rather than a higher mode. This conclusion is compatible with the regional geology, in that we may be observing either or both regeneration at the margin of the Keweenawan sedimentary wedge or reflection from the main boundary fault (Douglas Fault) of the Midcontinent Gravity High. Either of these possibilities leads to significant conclusions with respect to regional geology, regional velocity distribution, and local earthquake location.

4) Results of Seismicity Studies

Three local earthquakes have been observed during the time of operation of the Central Minnesota Seismic Array. These events fit nicely into a significant pattern of regional seismicity with excellent correlation to regional tectonics. A description of these relationships and their tectonic significance is presented in a paper by Mooney and Morey (1980).

A brief summary of these events is presented here:

Date	6 March 1979	16 April 1979	14 May 1979
Origin time	00h27m56.1s CUT	6h40m16.7s CUT	19h27m38.5s CUT
North Latitude	45°50'51"	46°41'48"	45°43'12"
West Longitude	93°44'53"	95°32'24"	92°59'31"
Depth	5 km	20 km	6 km
Magnitude	1.0	3.1	0.1
Location	Milaca, MN	Detroit Lakes, MN	Rush City, MN
Distance from CMSA-6	42 km	208 km	22 km
Azimuth from CMSA-6	268°	300°	134°

II. System Documentation and Routine Operation

1) System Description

A more detailed presentation of the following material will be found in Technical Report TR 1978-4: "System Documentation for Central Minnesota Seismic Array and Affiliated Stations".

The Minnesota earthquake recording system consists of the 6-element Central Minnesota Seismic Array (CMSA) plus 1-element stations at Minneapolis and Morris, MN.

All seismometers are 1 hertz vertical units. The CSMA seismometers are located on the circumference of a circle of diameter 27 km, with one at the center. Data are telemetered as FM signals via telephone to Minneapolis, approximately 100 km south, where they are recorded on a 7-channel magnetic tape recorder. The 7th channel is used for WWVB time code. One channel is continually displayed on a visual recorder for monitoring. The tapes are played back onto a 7-channel visicorder, with a wide range of options in playback speed.

The Minneapolis station consists of one seismometer located in a mine about 8 km from the Minneapolis campus of the University of Minnesota. Data are telemetered to the campus where they are displayed on a visual recorder.

The Morris station consists of one seismometer located in a vault about 12 km from the Morris campus of the University of Minnesota. Data are telemetered to the campus where they are displayed on a visual recorder.

The latter two stations relay on WWV/WWVB time code, with synchronization to a local chronometer.

Typical amplification for the CMSA stations is 50K or 100K at 1 hertz, depending upon amplifier setting on the playback system. Amplification for Morris is comparable, and is lower by a factor of 2-4 for Minneapolis.

CMSA and the Minneapolis station have been operating with some interruptions since 1 January, 1977. The Morris station operated for two months in spring, 1978, but was re-located to a less noisy site in July, 1978.

Location data for the Minnesota stations are presented in Table I. The stations are shown on the map of Figure 1.

System amplification is shown in Figure 2. This represents the ratio, displacement on the final playback record divided by earth displacement at the seismometer. Two variables enter into the calibration curve shown in Figure 2, namely the preamplifier gain and the playback amplifier setting.

The curves are shown for a standard preamp gain setting of 88 db. Other settings require multiplication by appropriate factors: for example, a setting of 82 db requires multiplication of the curve by 2.0.

Two curves are shown for playback amplifier settings of 0.1 and 0.2. For other settings, the 0.1-curve values should be multiplied by (setting) /0.1.

Table 1: Minnesota Seismic Station Locations

Code	Station Number	Latitude, north	Longitude, west	Elevation Meters	Elevation Feet
CM1	1	45°56' 1.32"	93°21' 9.96"	324.6	1065
CM2	2	45°58'26.76"	93°09'42.42"	323.1	1060
CM3	3	45°52'28.98"	93°00'34.98"	294.1	965
CM4	4	45°45'00.00"	93°06' 7.02"	298.7	980
CM5	5	45°46'58.92"	93°19"24.18"	298.7	980
CM6	6	45°51'35.58"	93°11'51.78"	310.9	1020
MFM	Ford Plant, St. Paul, MN	44°54'50.7"	93°11'34.9"	225.5	740 seismometer
				245.7	806 surface
				20.1	66 depth below surface
MRM	Morris, MN	45.8758°	95.8109°	358.8	1177

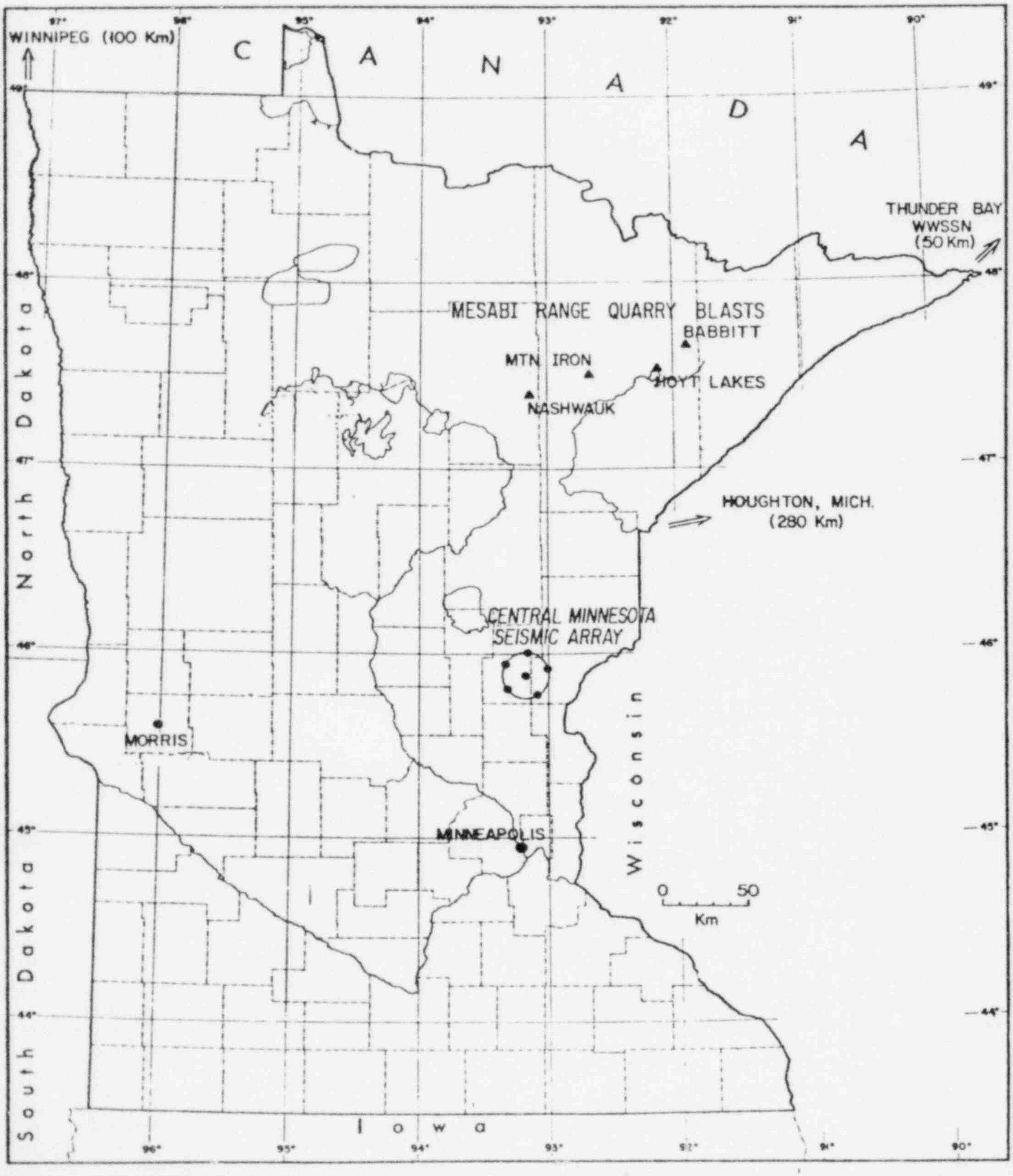

Figure 1: Location Map for Minnesota Seismic Stations

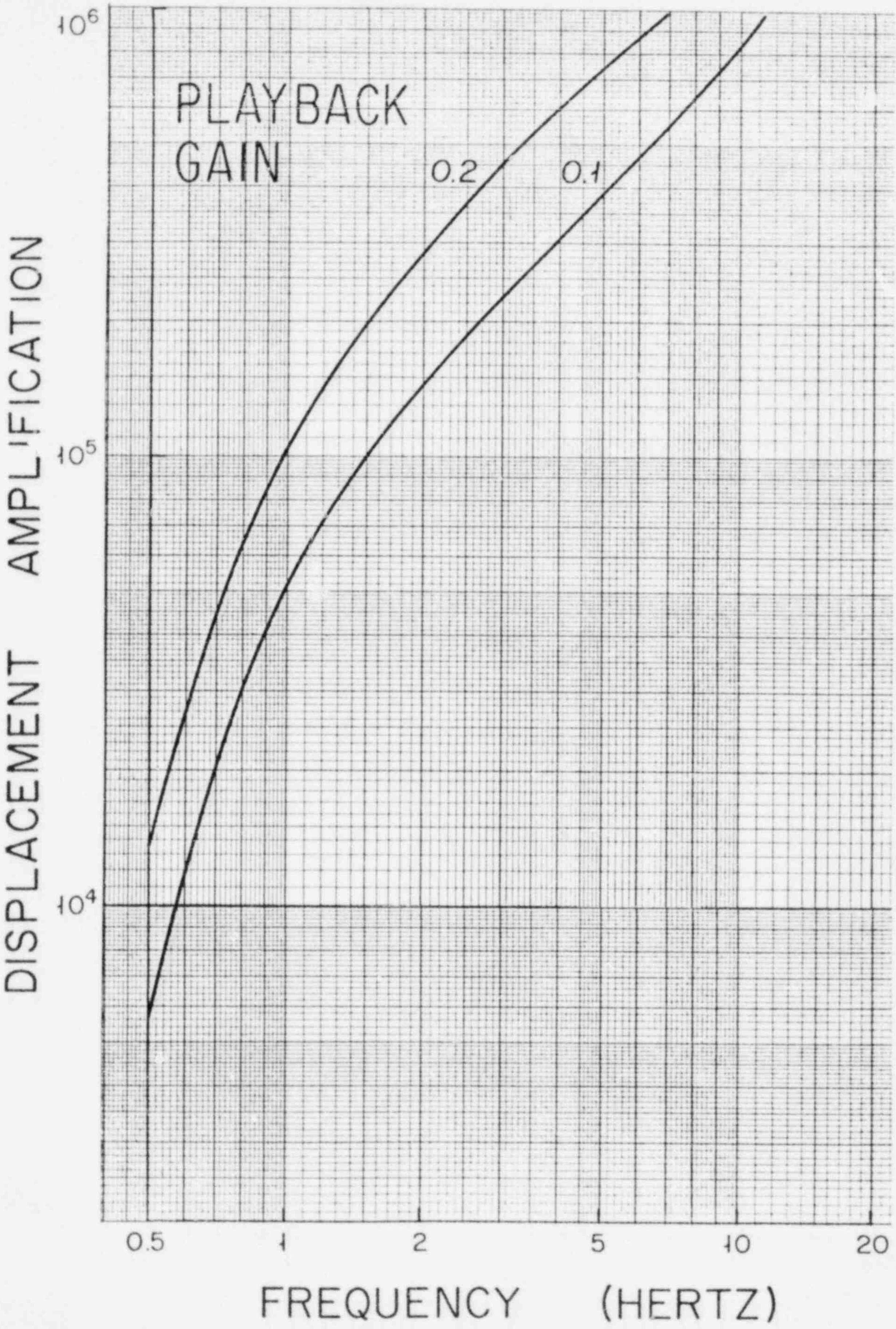

Figure 2: Displacement Amplification vs Frequency for CMSA Stations

2) Geologic setting for the Central Minnesota Seismic Array Midcontinent Gravity High. This location was chosen for two reasons: (1) The array should then be able to detect even minor activity, if any occurs, on the western boundary fault (Douglas Fault), and (2) Excellent geologic control is available on upper crustal structure through a large number of completed refraction seismic profiles (Mooney et al, 1970).

Figure 3 shows the location of the CMSA in relation to a Bouguer gravity map of east-central Minnesota. The contours define the Midcontinent High at these latitudes. Figure 4 shows the CMSA with reference to an aeromagnetic contour map.

Figure 5 shows in greater detail the CMSA location with reference to the Douglas Fault defining the western margin of the Midcontinent Gravity High and to the western flanking sedimentary basis. The relationship can be seen more clearly on Figure 6, a geologic cross section along line BB' of Figure 5 as inferred from the seismic refraction profiles.

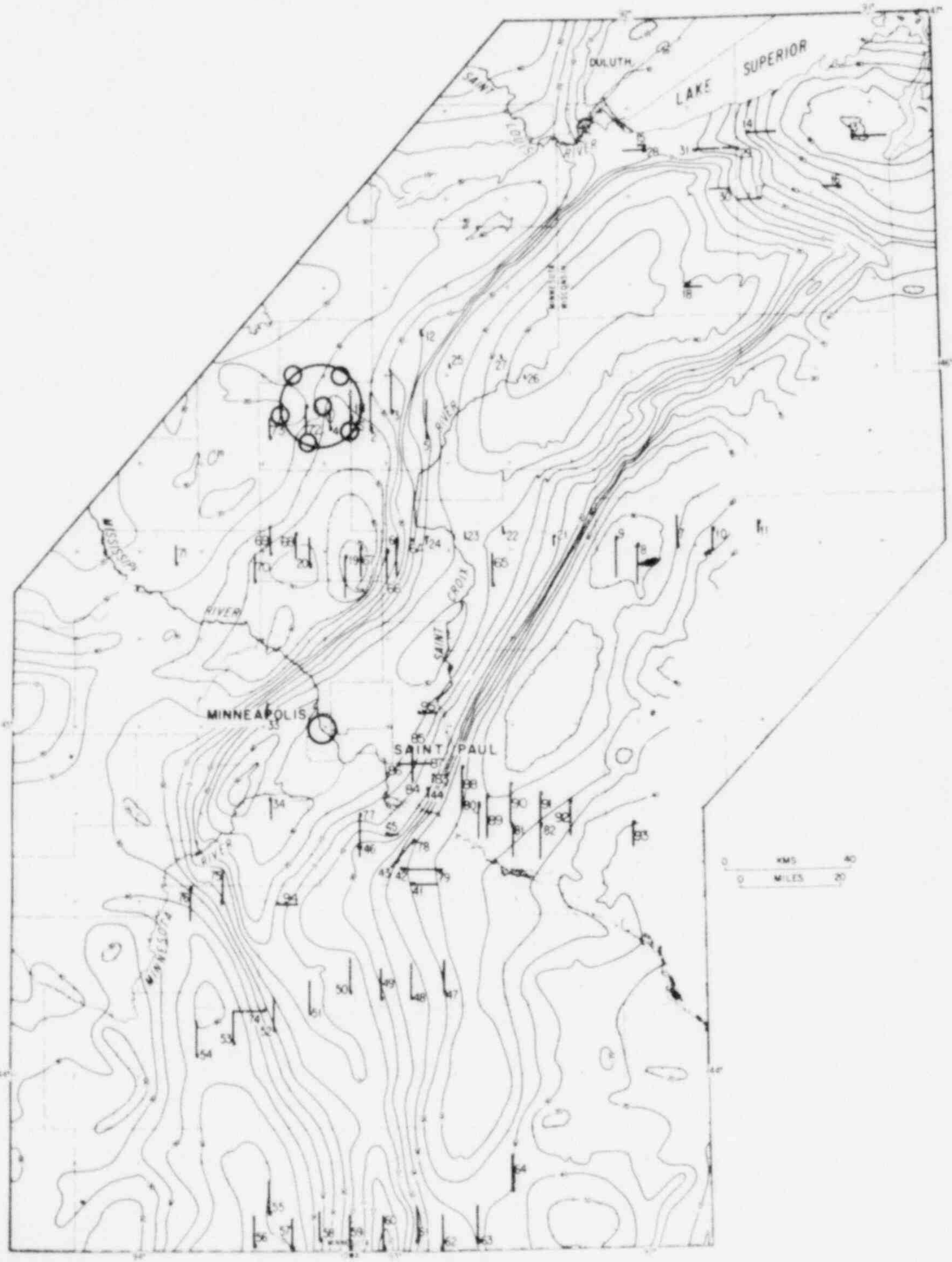

Figure 3: Bouguer Gravity Map of East-central Minnesota showing Location of CMSA and of Refraction Seismic Profiles

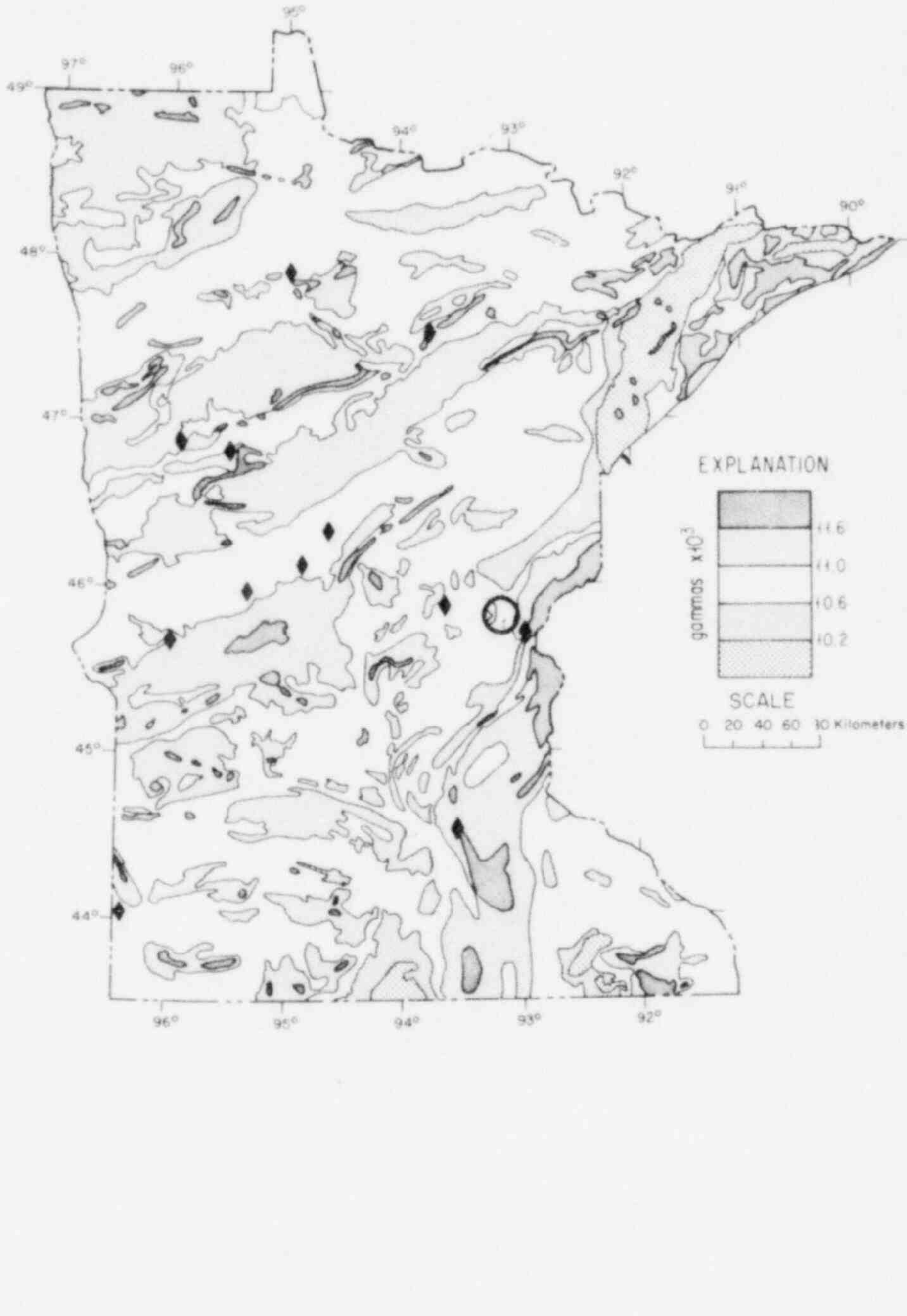

Figure 4: Aeromagnetic Map of Minnesota, Showing Location of CMSA and Historical Seismicity as Described in Section IV.2.

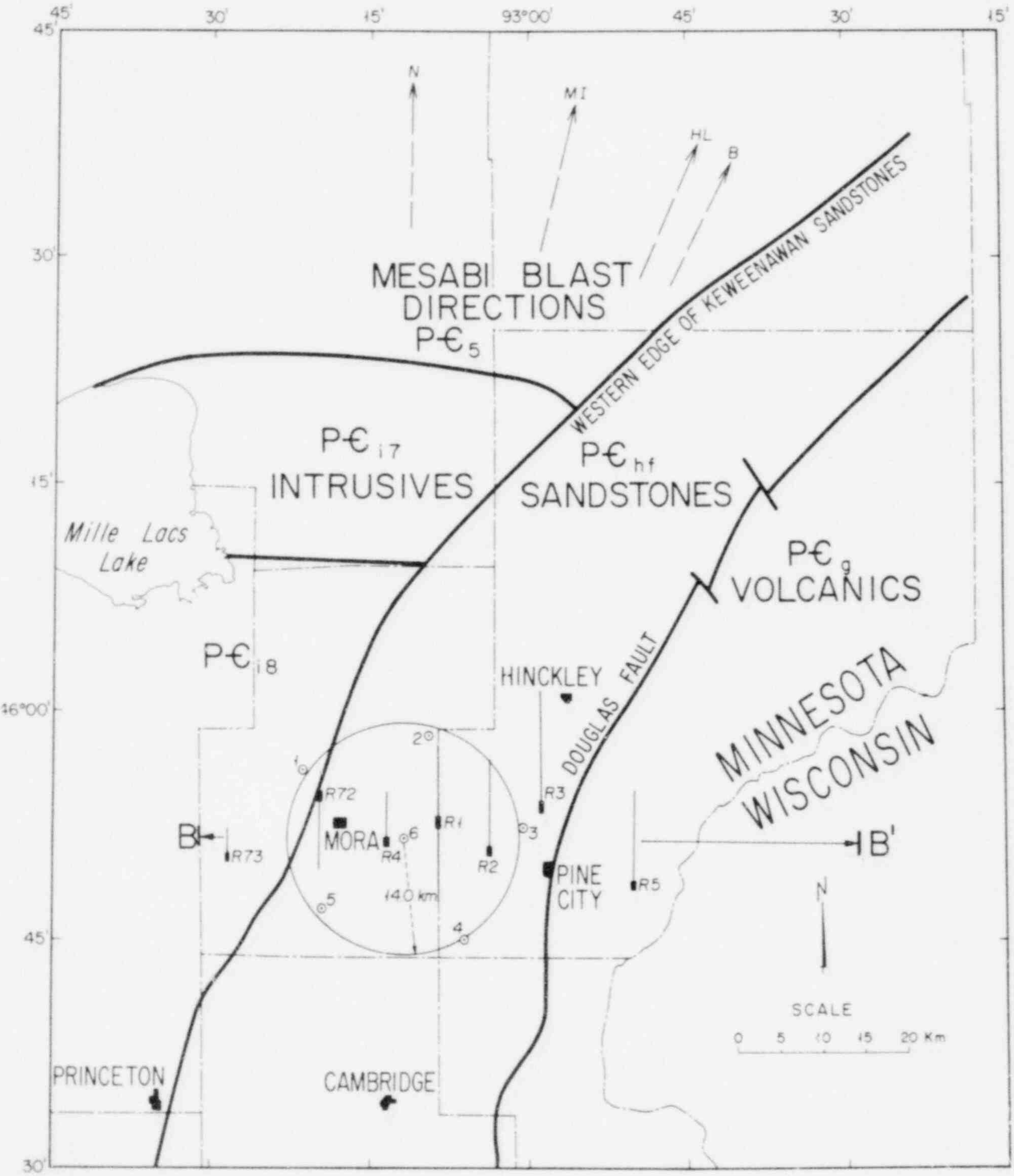

Figure 5: CMSA Locations with Reference to Regional Geology and to Refraction Seismic Profiles (R1,R2,etc)

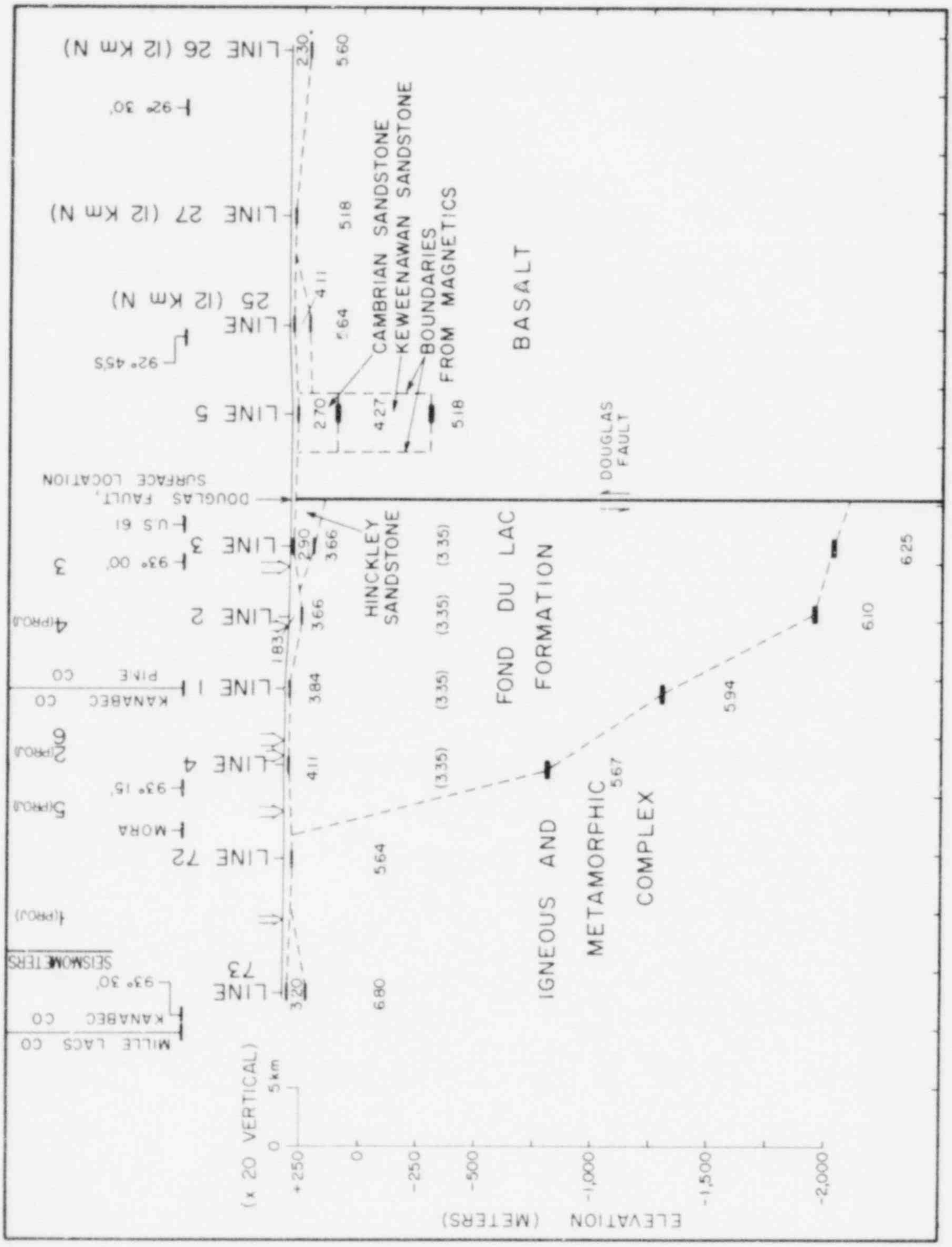

Figure 6: CMSA Locations Projected onto Geologic Cross Section BB' of Figure 5

3) Operating Procedures and Sample Seismic Waveforms

A more detailed presentation of the following material will be found in Greenhalgh (1979) and Mosher (1980).

Figures 7 - 9 show the array configuration, starting from individual station layouts and proceeding through multiplexing/transmission/demultiplexing to the 7-channel tape recorder. A separate tape recorder for playback provides flexibility in time and amplitude scaling. Common-time-base recording permits measurements of relative arrival times across the array to high precision, and simultaneous WWVB time code recording yields absolute time.

The first playback is carried out at high time compression to identify events. Typically this yields one hour of real time on 6 cm of chart paper. Events are identified by simultaneous blips on two or more channels. Tests show that events with duration greater than 2 seconds can be recognized, depending somewhat upon signal to noise ratio. Confirmation and cross-check is provided by recording one of the traces continuously on a Sprengnether drum recorder at 60 mm/minute. Detailed tests of this combined detection method (Greenhalgh, 1979) show that it misses few events.

The criterion of simultaneity on two or more channels eliminates as events virtually all cultural and meteorological noise, since these will affect only one element of the array or at worst will propagate across the array at a very low apparent velocity.

The events which fulfill the criterion of detection are then played back at high speed. Normal playback yields 1 second of real time for 1 cm of chart paper, although four times this scale can be obtained if desired.

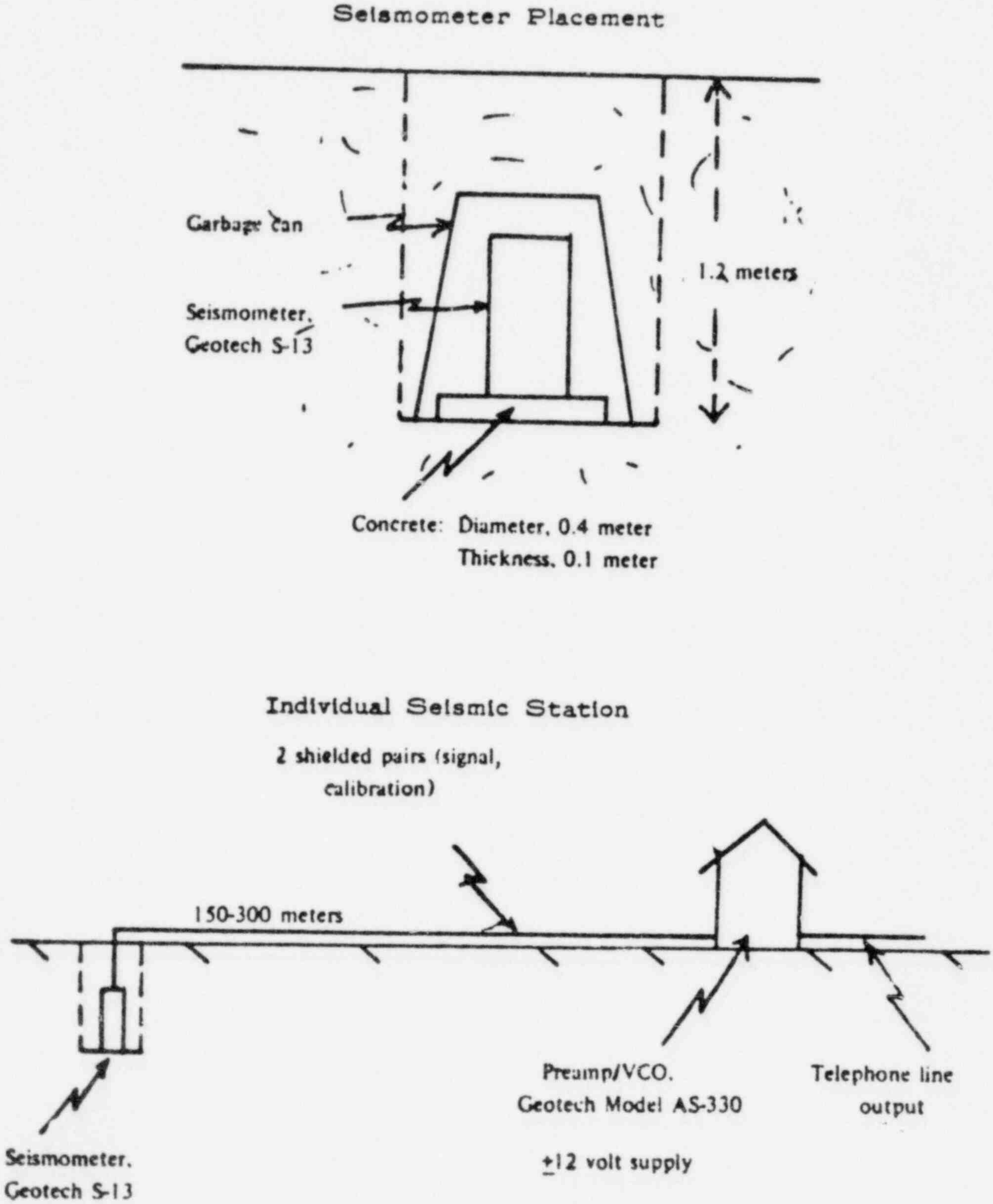

Figure 7: Individual Seismic Station Configuration

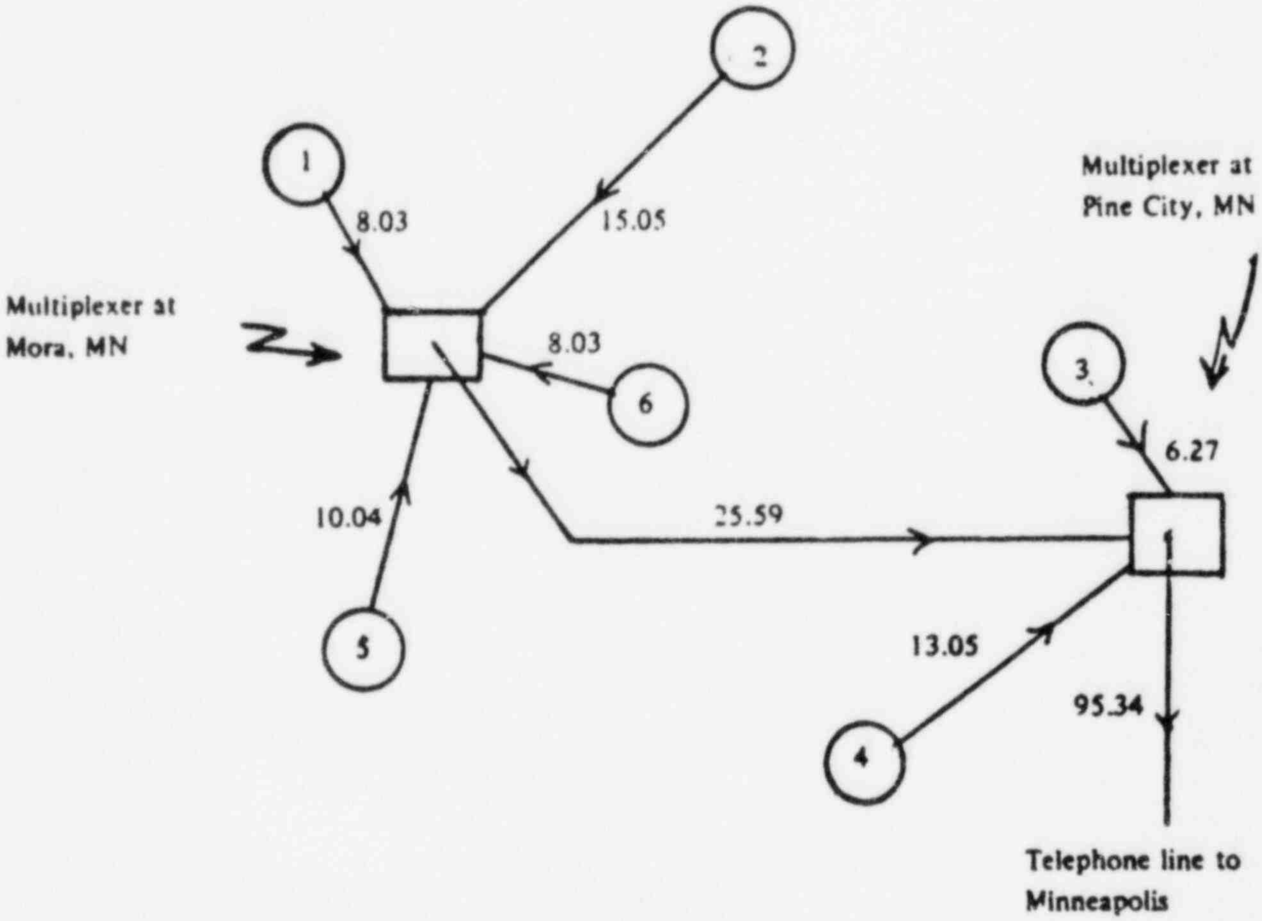

(Distances in kilometers, airline)

Figure 8: Multiplexer Configuration

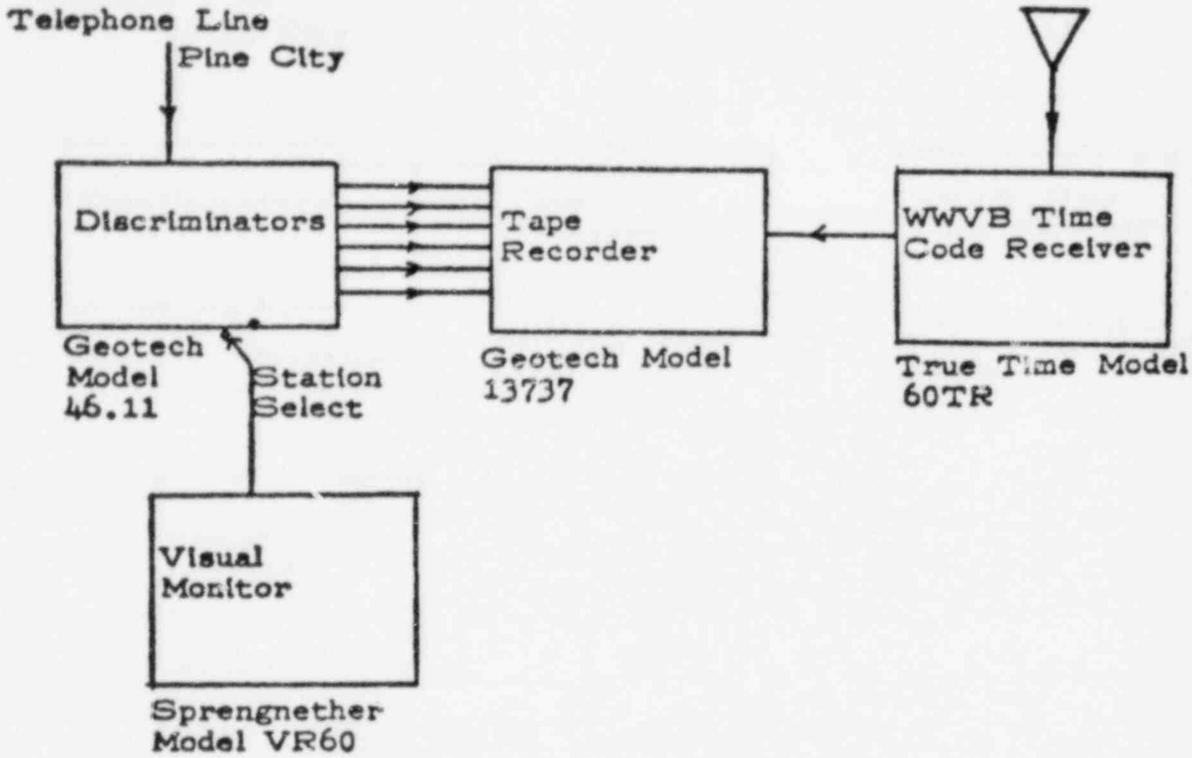

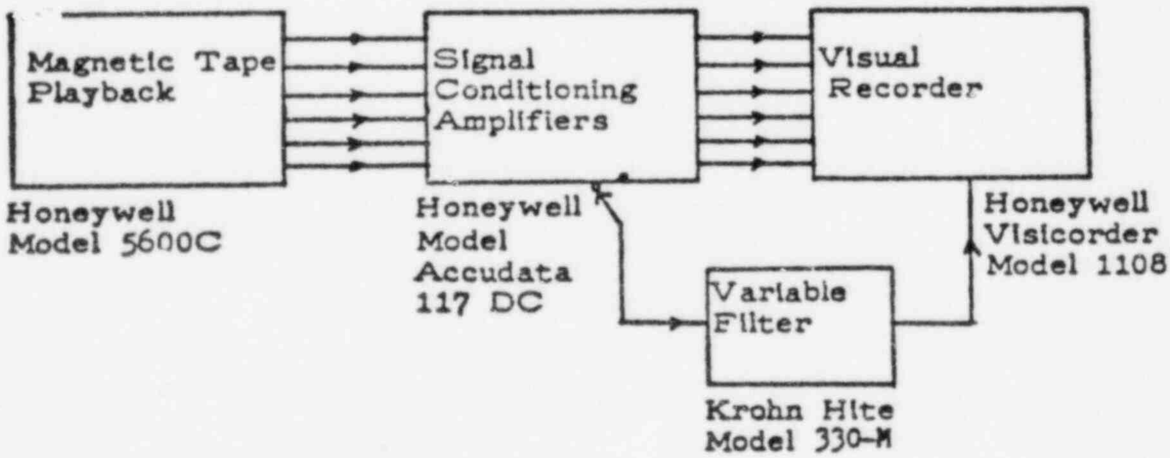

Figure 9: Recording and Playback Configurations

Figure 10 shows the array record written from an intermediate-depth earthquake on the Peru-Brazil border at a distance of 57.0°. It can be seen that moveout across the array is sufficient to permit accurate measurement of apparent horizontal velocity and azimuth of arrival. For interpretation of such data, we have preferred not to rely upon first-break time measurements alone. Instead, we take advantage of waveform similarity across the array by tracing several cycles from one station and matching it against other stations. The resulting time shifts can be supplied to a computer program containing station coordinates, to yield an output of apparent horizontal velocity and/or slowness, arrival azimuth and standard deviations for both.

Three seismic arrivals can be seen in the 40 seconds of record shown in Figure 10. The phase inversion of pP can be recognized. The benefits of multiple-trace display on a common time base are clearly displayed in this record, where the individual pP and PcP arrivals might be difficult to identify on any one of the traces alone. When viewed across the total record, however, the distinctive characteristics of the pulse permit easy identification.

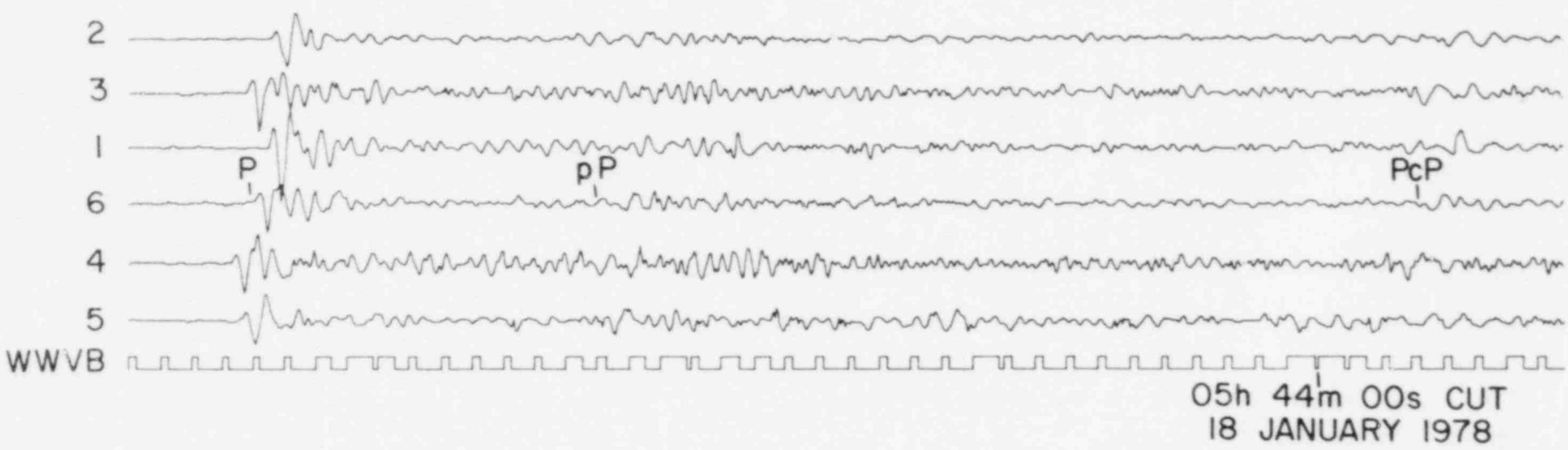

Figure 10: Playback of Teleseismic Event (Peru; h = 170 km; M = 5.0)

Figure 11 shows the array record written from a mine blast on the Mesabi Iron Range. This particular blast was 162,540 pounds of explosive at the National Steel Company mine at Keewatin, Minnesota. Epicentral distance is 174.3 km.

This record displays some of the features which are commonly observed at CMSA from large mine blasts. The P arrival is often emersio and the S arrival even more so. High frequencies are often present. Surface waves with periods 1-2 seconds may attain large amplitudes.

We should emphasize, however, that Mesabi mine-blast records show wide variability, presumably due to source effects (amount and type of explosive, rock coupling, delay patterns, etc). We observe i or e P arrivals, occasionally i S arrivals, long or short period P and S, pulse-like or prolonged P and S. We observe large body waves with neglible surface waves, or the reverse. We observe large P and small S, or the reverse. Each mine produces a different pattern of surface waves, such that we can usually identify the mine from this feature alone.

Figure 12 shows an example of a very long period P arrival, from an Erie Mining Company blast on the Mesabi Iron Range, at a distance of 207.5 km. Array records from local earthquakes will be shown in a later section.

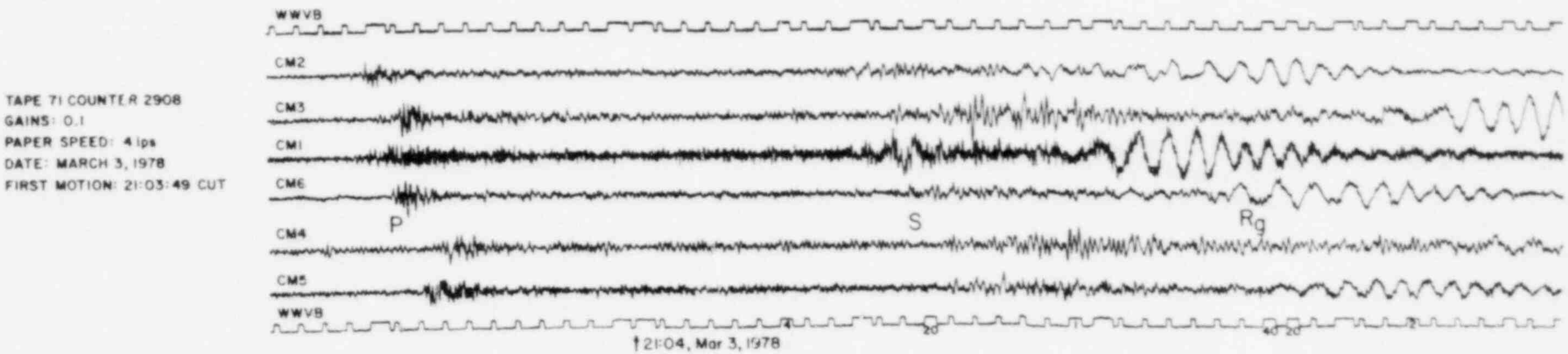

Figure 11: Mesabi Mine Blast Record at Distance of 174.3 km

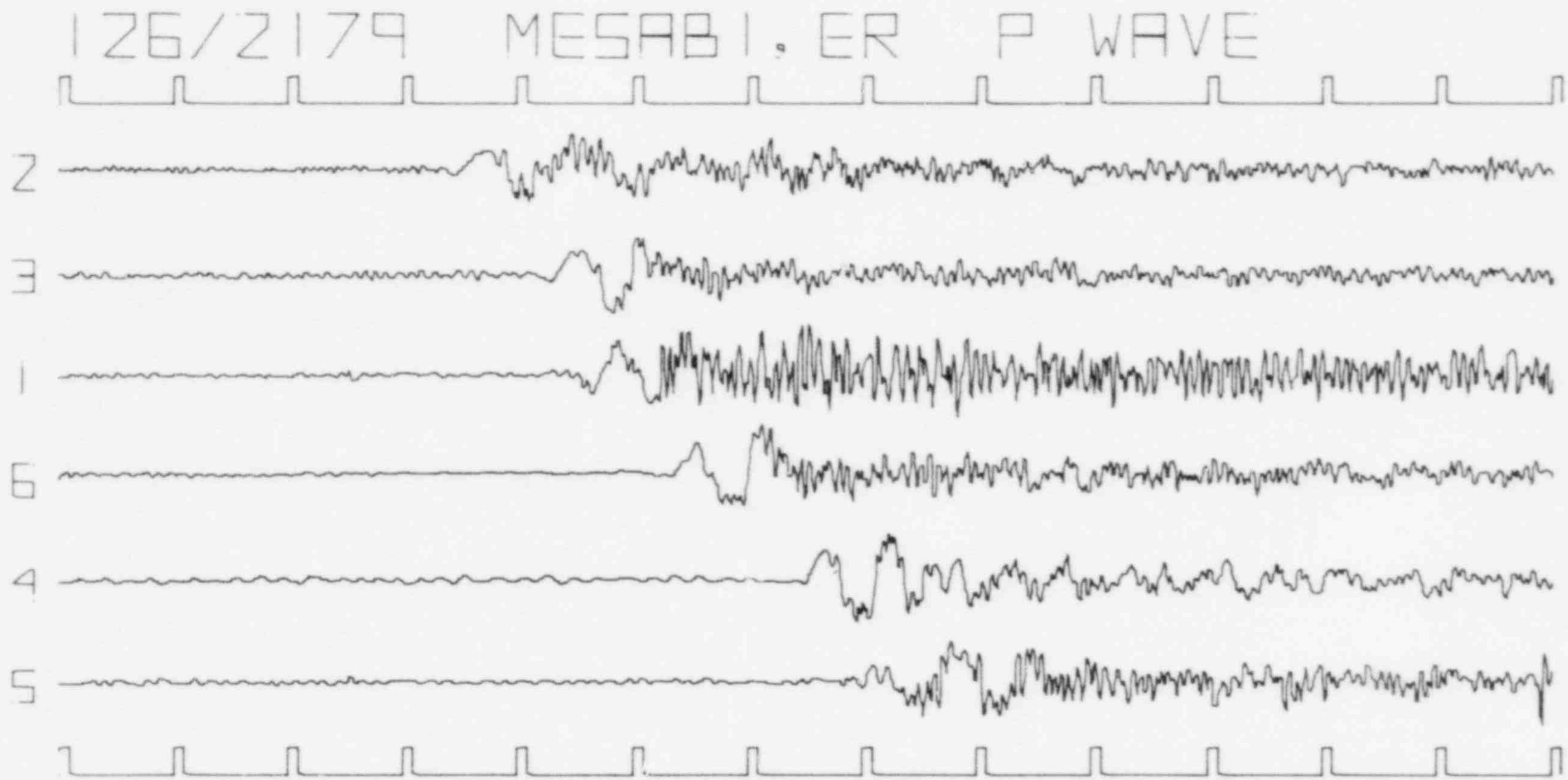

Figure 12: Long-Period P Wave Arrivals from a Mesabi Mine Blast at 207.5 km

4) Location of mines and quarries used in calibration

A more detailed presentation of the following material will be found in Technical Report TR 1978-2; "A Study of Mine Blasts for Magnitude Calibration for the Central Minnesota Seismic Array".

The Central Minnesota Seismic Array records ground vibrations transmitted from numerous regional mines and quarries, at distances up to 350 km. Some of these blasts involve unusually large amounts of explosive. For example, Reserve Mining Company in Babbitt, Minnesota sets off blasts up to 2.5×10^5 kg (600,000 pounds). Even at the Reserve distance of 220 km, such blasts may suffice to saturate the CMSA recording system.

Mine locations are listed in Table 2. The map in Figure 13 shows geographical relationships between CMSA and the Mesabi mines.

Table 2: Mine and Quarry Locations Used for Array Calibration

	N. Lat	W. Long.	Dist to CMSA-6 km	Azimuth
Mesabi Iron Range, Minnesota				
Butler Taconite, Nashwauk MN	47.363	93.222	167.1	359.30
National Steel, Keewatin MN	47.429	93.058	174.3	3.45
Hibbing Taconite, Hibbing MN	47.462	92.955	179.1	5.86
Eveleth Taconite, Eveleth MN	47.450	92.548	185.9	15.30
U.S. Steel, Mountain Iron MN	47.533	92.650	190.6	12.49
Erie Mining, Hoyt Lakes MN	47.582	92.196	207.5	22.46
Reserve Mining, Babbitt, MN	47.690	91.958	220.4	25.00
Marquette Iron Range, Michigan				
	45°59.5'	87°59'	404.67	86.05
	46°27'	87°37'	436.00	79.34
	46°24'	87°59'	407.36	79.65
	46°27'	87°38'	434.73	79.32
Minnesota				
Shiely Quarry, St. Cloud MN	45.55	94.24	88.2	247.40
Wisconsin				
Dresser Traprock Co, Dresser WI	45.37	92.63	70.5	140.69
Jackson County Iron Co, Black River Falls WI	44.32	90.75	257.7	130.70
Ontario				
Steep Rock Iron Mines, Atikokan, Ontario	48.82	91.65	348.9	19.02

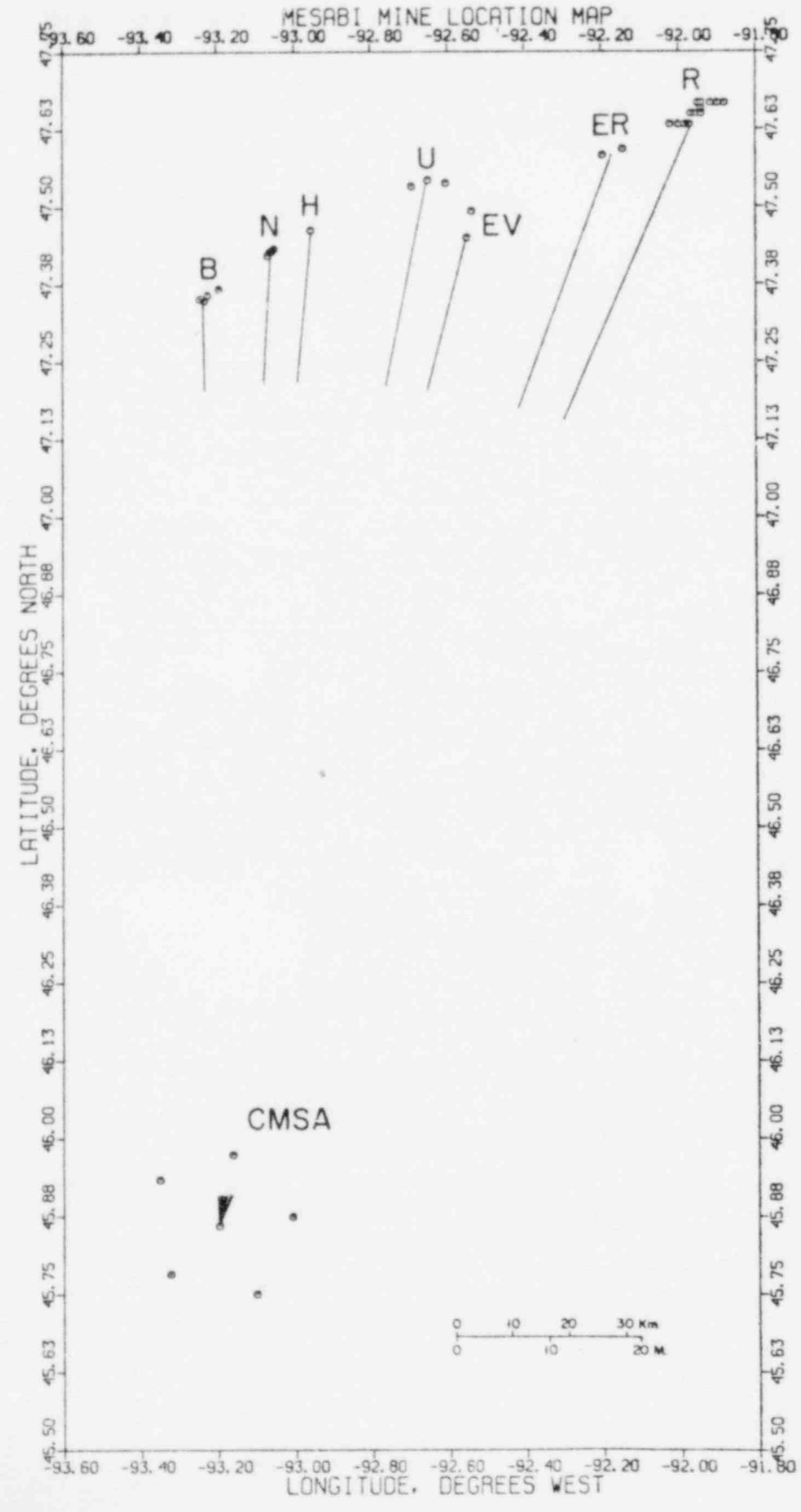

Figure 13: Mesabi Mine Locations in Relation to CMSA

5) Seismic Event Logs

Seismic Event Logs were published for CMSA events from 1 January, 1977, through 31 March, 1979. Sample formats are shown in Figure 14 for teleseismic events and in Figure 15 for mine and quarry blasts. These figures are extracted from Technical Report TR 1979-5: "Seismic Event Log for Central Minnesota Seismic Array: 1 January 1979 to 31 March 1979".

The event logs served an important purpose for system documentation and calibration during the first two years of operation. They are no longer needed and have been discontinued as of 1 April, 1979. They will be replaced by individual reports on local and regional events as they occur.

Despite the termination of published Event Logs, an informal log is compiled internally at the University of Minnesota for all events from whatever source. A complete collection of seismic waveforms for all events is maintained also. These are stored as playbacks on Kodak Linagraph Direct Print Paper. The original magnetic tapes are recycled on a six month rotation hence they remain available for six months after the event. A few selected waveforms have been digitized for special study and are retained in storage.

1979	PHASE	ARR TIME	CALC AZ	CALC VA	LOCATION	O TIME	LAT	LONG	H	M	DIST	AZ	SLOWN
JAN 1	IP,UP	23 19 40.0	246.30+-1.63	10.89+-0.38	CALIFORNIA	23 14 39.0	33.93	-118.70	6		22.80	247.51	9.88
JAN 6	IP	01 41 28.2	162.25+-1.99	14.64+-0.48	PERU	01 31 48.1	-8.87	-75.76	29	5.7	56.69	159.21	7.09
JAN 8	EP	16 10 45.0			ANDREANOF ISL.	16 01 50.3	51.63	-173.16	40	4.8	50.56	307.44	7.51
JAN 10	IP,DN	04 35 31.8	194.35+-0.39	13.59+-0.17	MEXICO	04 29 26.5	15.75	-96.47	47	5.2	30.15	186.30	8.87
JAN 10	IP,DN	13 29 58.7	155.38+-15.47	17.49+-7.44	MEXICO	13 24 16.9	16.99	-93.35	168	5.7	28.79	180.29	8.89
JAN 11	EP	06 47 34.4			SOUTH SUMATRA	06 28 15.0	-4.15	101.08	33	5.5	136.63	339.18	1.90
JAN 12	EP	04 05 15.3	123.12+-18.33	20.41+-4.45	GUATEMALA	03 59 02.9	14.32	-91.48	86	5.5	31.47	176.80	8.78
JAN 12	IP,UP EPCP	14 58 44.9 14 59 31.5	87.33+-6.19	14.09+-1.17	NORTH ATL OCEAN	14 49 06.1	35.56	-17.11	33	5.3	56.56	71.43	7.09
JAN 14	IP,UP	19 28 12.4	98.90+-14.75	12.22+-3.53	COLOMBIA	19 20 28.1	6.70	-72.89	132	5.3	42.79	149.46	8.03
JAN 16	EP	07 21 58.7	288.50+-27.56	15.33+-6.76	FOX ISLANDS	07 13 31.2	52.77	-167.86	32	5.1	47.13	306.97	7.77
JAN 16	EP IPCP I(P)P	10 03 39.5 10 03 42.8 10 04 01.7			IRAN	09 5[illegible] [illegible]1.6	33.70	59.57	33	5.4	97.07	22.52	4.57
JAN 17	IP,DN	08 12 12.1	25.42+-6.37	21.25+-4.78	KAZAKH SSR	07 59 56.9	47.99	48.21	0	6.0	80.63	25.06	5.35
JAN 17	IP I(P)P	19 20 06.8 19 20 17.5			KAMCHATKA	19 09 40.4	53.04	159.88	33	5.3	63.43	319.85	6.62
JAN 18	IP,UP I	14 08 34.4 14 08 46.5			EAST INDIES	13 50 38.7	-7.24	122.97	555	5.3	130.48	309.98	

Figure 14: Sample Seismic Event Log for Teleseismic Events Recorded on CMSA

1979	PHASE	CM6 ARR TIME	MINE(TENTATIVE)	COMMENTS	TAPE
JAN 11	EP	17 07 20.0	MICHIGAN		122/0783
JAN 11	IP	12 15 54.5	U S STEEL	GOOD P WAVES	122/0787
JAN 11	IP	21 13 25.5	MESABI	LARGE P GOOD SURFACE WAVES	122/0897
JAN 12	EP	16 02 13.0	MICHIGAN		122/1424
JAN 12	EP	17 04 50.0	MICHIGAN		122/1452
JAN 12	IP	17 52 16.1	BUTLER		122/1476
JAN 12	IP	18 22 49.3	RESERVE		122/1490
	IS	18 23 14.5			
JAN 13	EP	17 08 09.0	BLACK RIVER FALLS	EXCELLENT SURFACE WAVES ON CMS	122/2127
JAN 15	EP	17 03 05.0	MICHIGAN	GOOD ARRIVALS ON CMSA-1,3	123/0126
JAN 15	IP	19 42 21.8	U S STEEL	LARGE P WAVES	123/0200
JAN 16	IP	17 55 40.1	U S STEEL	HIGH FREQUENCY SIGNALS	123/0822
JAN 16	IP	19 38 32.9	U S STEEL	HIGH FREQUENCY SIGNALS	123/0870
JAN 16	EP	21 05 35.0	MICHIGAN		.23/0911
JAN 17	EP	17 15 20.0	MICHIGAN		123/1476
JAN 17	IP	19 14 29.4	NATIONAL	GOOD P,SURFACE WAVES	123/1531
JAN 18	IP	16 56 38.5	BUTLER	GOOD RECORD	123/2139

Figure 15: Sample Seismic Event Log for Mine and Quarry Blasts Recorded on CMSA

III. System Calibration and Regional Geologic Studies

1) Detection capability of the Central Minnesota Seismic Array

A more detailed presentation of the following material will be found in Greenhalgh (1979).

A crucial specification for the CMSA is given by the lower limit of earthquake detection capability expressed as a function of magnitude and epicentral distance.

The most direct evidence can be obtained from local earthquakes of known magnitude and epicentral location. Three such events have been detected on the CMSA, as follows:

6 March 1979	$m_b = 1.0$	X = 42 km from CMSA-6
16 April 1979	3.1	208
14 May 1979	0.1	22

Further data on these events including reproductions of the CMSA seismograms are presented in section IV.1. The seismograms show that all three were recorded with good signal-to-noise ratio. We conclude that these magnitude-distance combinations must lie well above the level of detection capability.

A second approach can be made through system response curves combined with an analysis of representative noise levels on CMSA. Greenhalgh (1979) presents results of this analysis but we will not reproduce them here since they do not lead to tight constraints on detection capability.

A third approach can be made by comparing the CMSA Station Log of observed events with catalogs of earthquakes or mine blasts. The reasoning here is that some events will have been detected by CMSA whereas others will not. The boundary between these two categories, expressed as a function of magnitude and distance, will delineate a rough level of detection capability.

Figures 16 - 18 show results for this third type of analysis. They suggest that the limit of detectability for teleseism ranges from $m_b = 4$ at $\Delta = 20^{\circ}$ to 5 at 90°. For regional events, the distance range of data is limited but a cutoff of $m_b = 3.5$ at a distance of 1600 km is suggested. For mine blasts, the detection limit seems to range from a ton of explosive at 100 km to 15 tons at 300 km., although these figures will clearly depend upon the delay pattern in the shooting.

Comparing the three approaches, we are led to conclude that the second and third are unduly pessimistic and that the detection capability for local earthquakes is greater than would have been predicted by them.

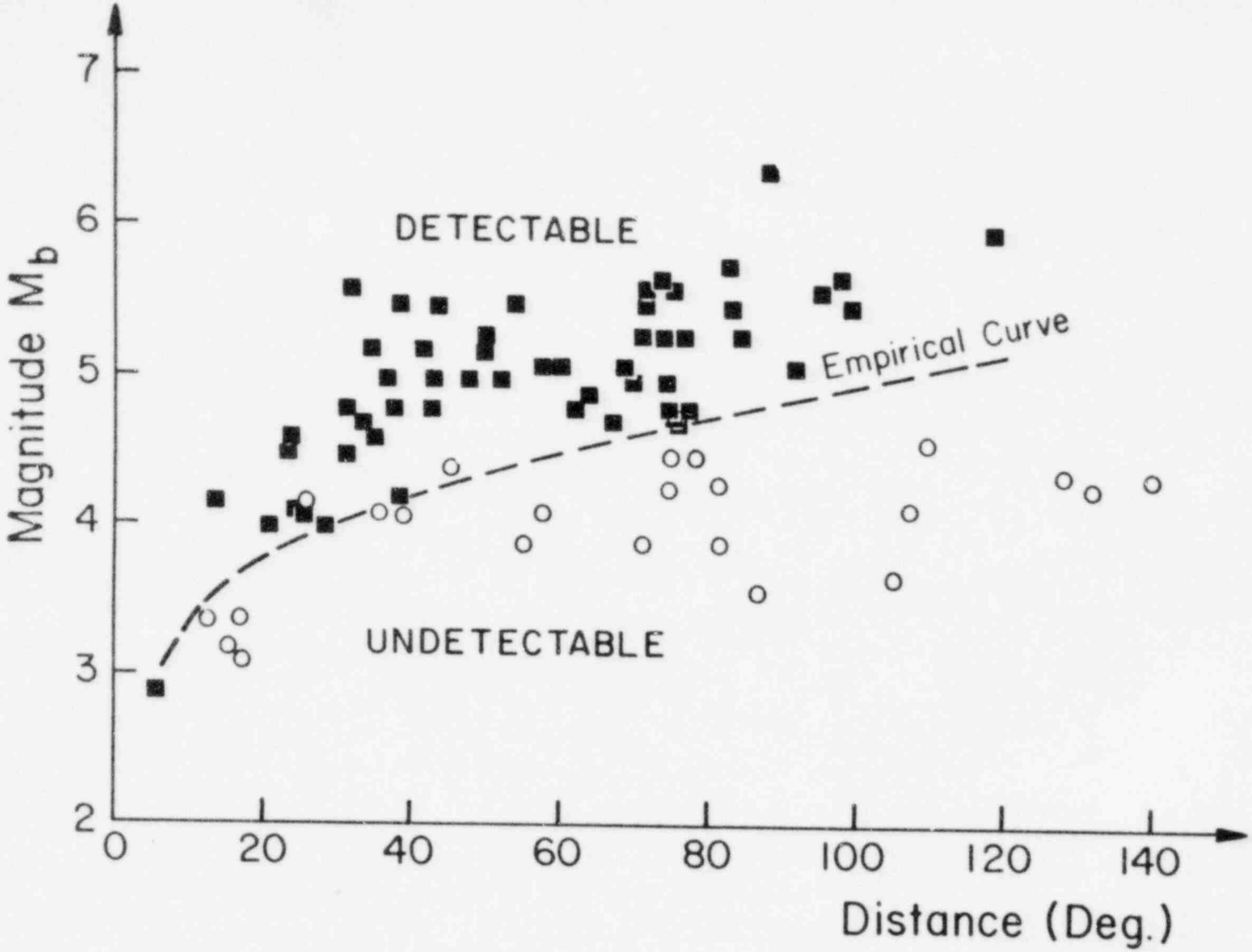

Figure 16: Teleseismic Detection Capability of CMSA

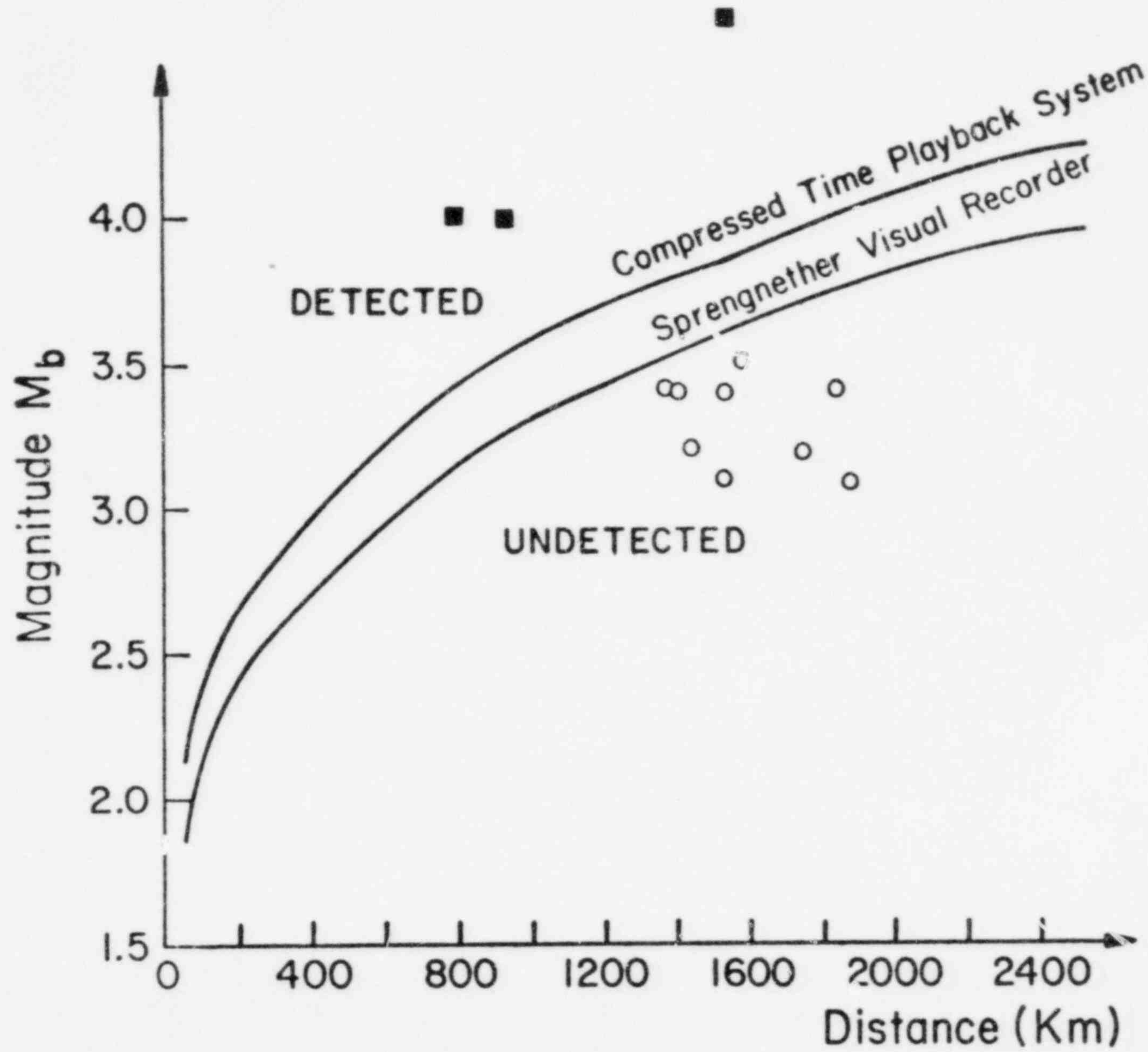

Figure 17: Regional Earthquake Detection Capability of CMSA
(Solid Lines are Based on Nuttli's $m_b(L_g)$ Formula)

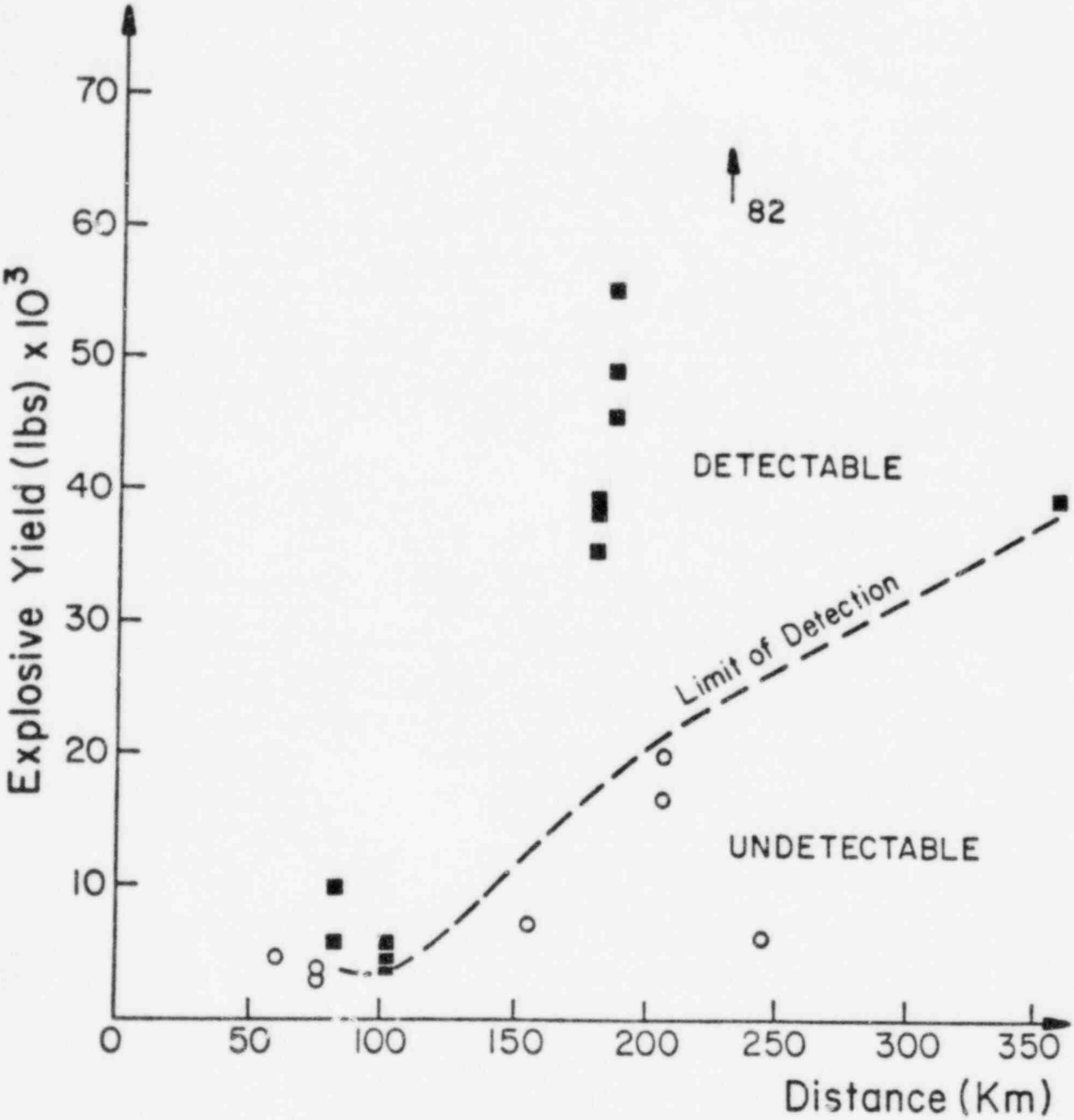

Figure 18: Mine and Quarry Blast Detection Capability of CMSA

2) Station Residuals and Array Bias

A more detailed presentation of the following material will be found in Greenhalgh (1979); Technical Report TR 1978-1: "A Study of Array Bias and Its Removal for the Central Minnesota Seismic Array"; and Technical Report TR 1979-1: "A Study of Array Bias (Revised) for the Central Minnesota Seismic Array".

The purpose of measuring stations residuals is twofold: 1) to obtain station corrections by which to improve location and detection capabilities for the array, and 2) to infer geologic and velocity structure beneath the array.

The procedure consists in computing station residuals in the form,

$$t_{residual} = t_{observed} - t_{expected}$$

Applied to teleseismic events, the expected times are obtained from standard travel time tables such as Jeffreys-Bullen or Herrin, using distances and azimuths for hypocenters obtained from the U.S. Geological Survey Publication, Preliminary Determination of Epicenters.

We have used times relative to center station CMSA-6, thus obtaining relative times and depths only. Details of the procedures are given in references cited above.

Representative results are shown in Figures 19 and 20. These and similar figures for the other CMSA stations demonstrate that the residuals differ significantly between stations, but that they are largely independent of distance and azimuth.

Table 3 presents mean residuals and standard deviations for the five stations relative to station CMSA-6, based upon three different data sets. Consistency of the results is excellent.

Figures 21 and 22 show the improvements obtained in computing azimuth and apparent horizontal slowness following application of the residuals as corrections to the raw readings.

The geologic interpretation was undertaken by testing the hypothesis that most of the observed residuals can be accounted for by the sedimentary wedge structure shown in Figure 6. We computed the expected residuals for the simplified structural model shown in Figure 23. This figure shows also a comparison between observed values and those computed using three different values for the basal refractor velocity.

The results demonstrate the conclusion that nearly all of the observed residuals can be accounted for by known velocity variations in the upper 2-3 km beneath the array.

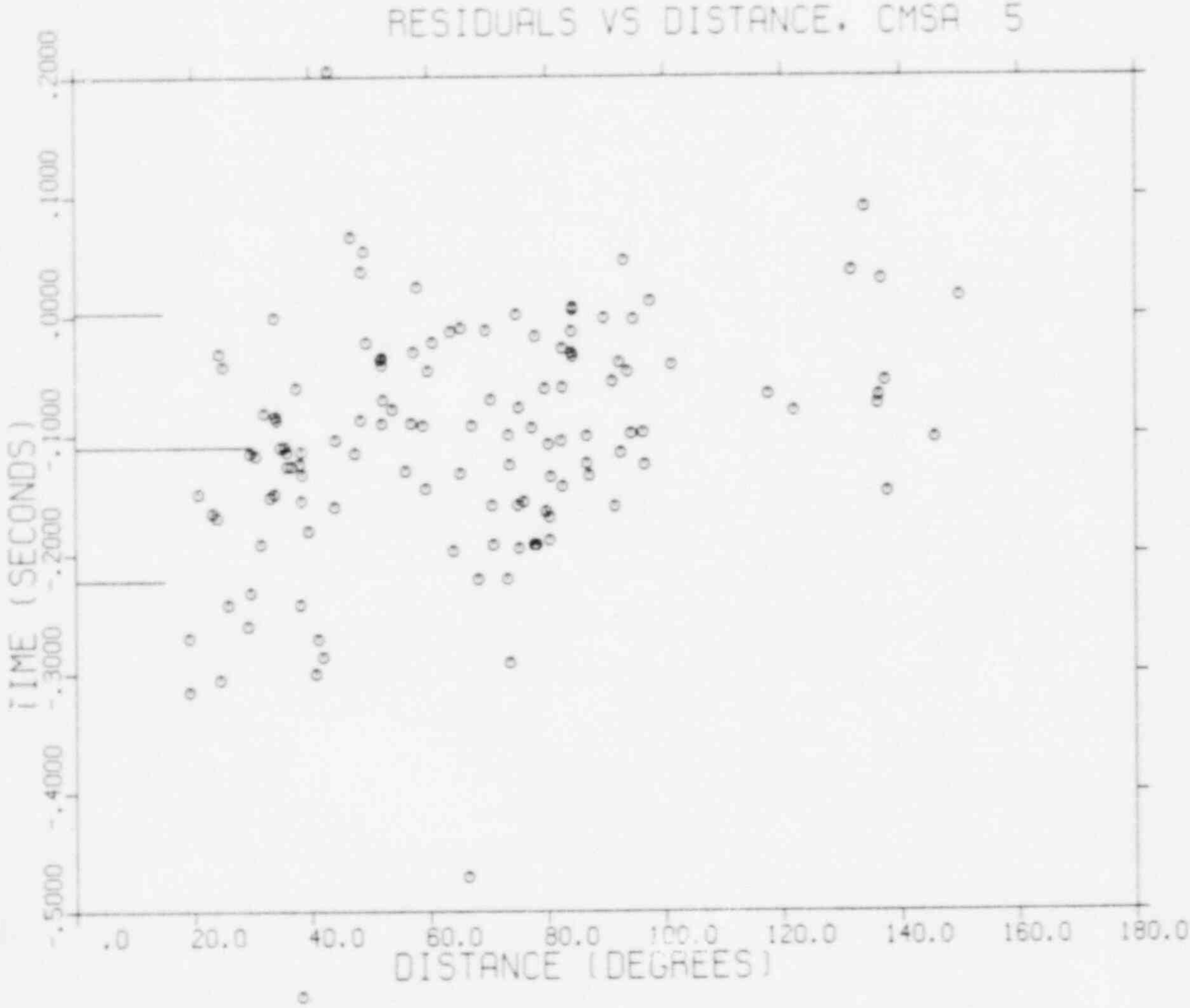

Figure 19: Teleseismic Residuals vs Distance for Station CMSA-5. Bars Show Mean and ±1 Standard Deviation.

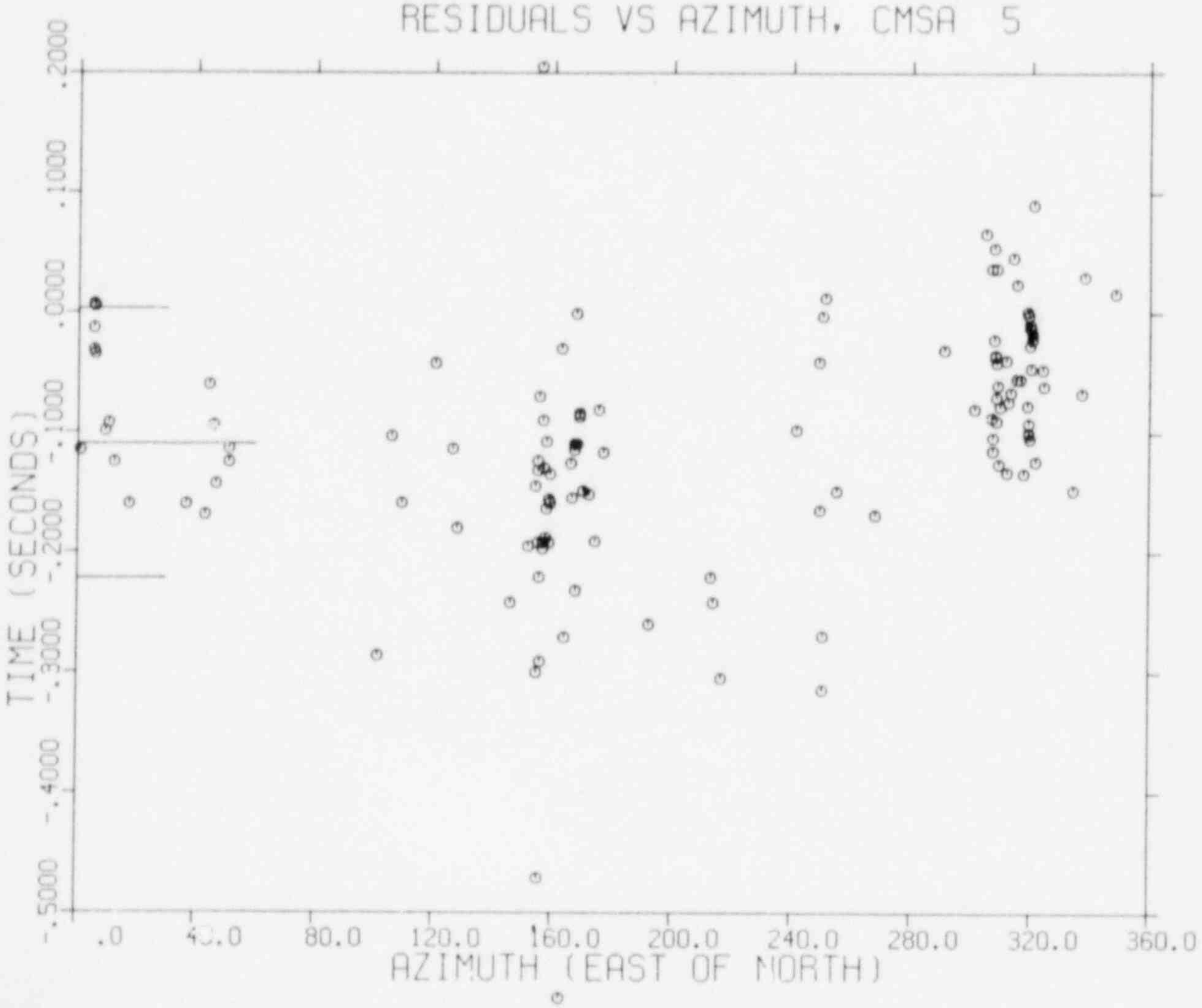

Figure 20: Teleseismic Residuals vs Azimuth for Station CMSA-5

Table 3: Summary of CMSA Station Residual Studies

( ) = number of data points. Readings in seconds.

Station	Mooney TR 1978-1 (52 teleseisms)	Greenhalgh, 1979 (85 teleseisms)	95% confidence limit for mean	Mooney, TR 1979-1 (164 teleseisms)
1	-.304±.107 (52)	-.325±.166 (70)	.039	-.317±.122 (145)
2	-.036±.110 (52)	-.058±.143 (60)	.036	-.060±.121 (155)
3	.027±.124 (52)	.051±.126 (72)	.029	.048±.112 (158)
4	.175±.095 (52)	.180±.143 (57)	.037	.179±.129 (155)
5	-.116±.091 (52)	-.116±.099 (55)	.026	-.110±.112 (131)
Time span	1 Jan to 31 Dec, 1977	1 Jan, 1977, to 31 May, 1978		1 Jan, 1977, to 15 Oct, 1978
Distance range	20-140°	20-140°		20-140°
Azimuth range	0-360°	0-360°		0-360°
Magnitude range	4.4-7.9	4.0-7.9		4.0-7.9

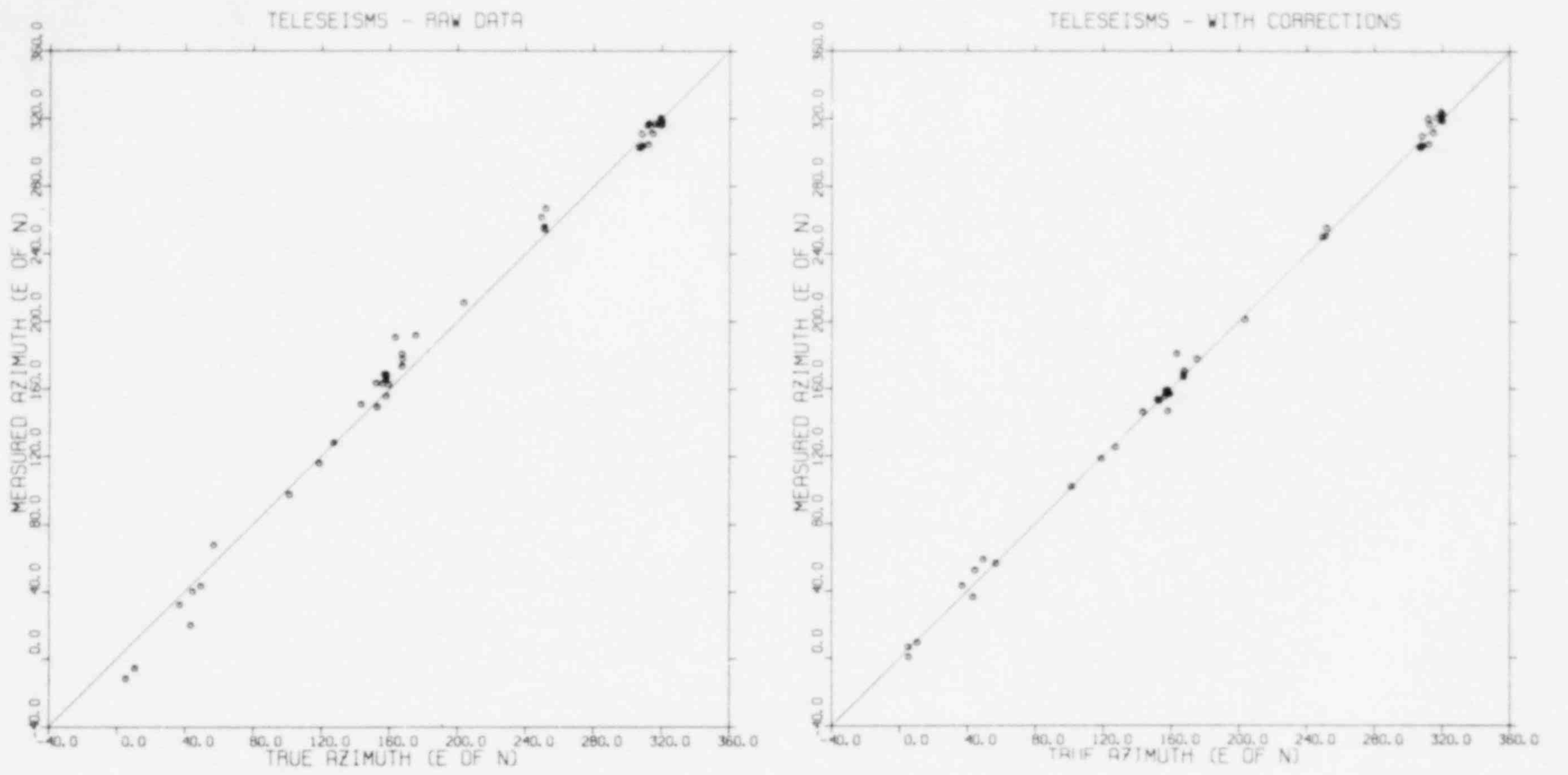

Figure 21: True vs Measured Azimuths, Before and After Applying Corrections Using Station Residuals

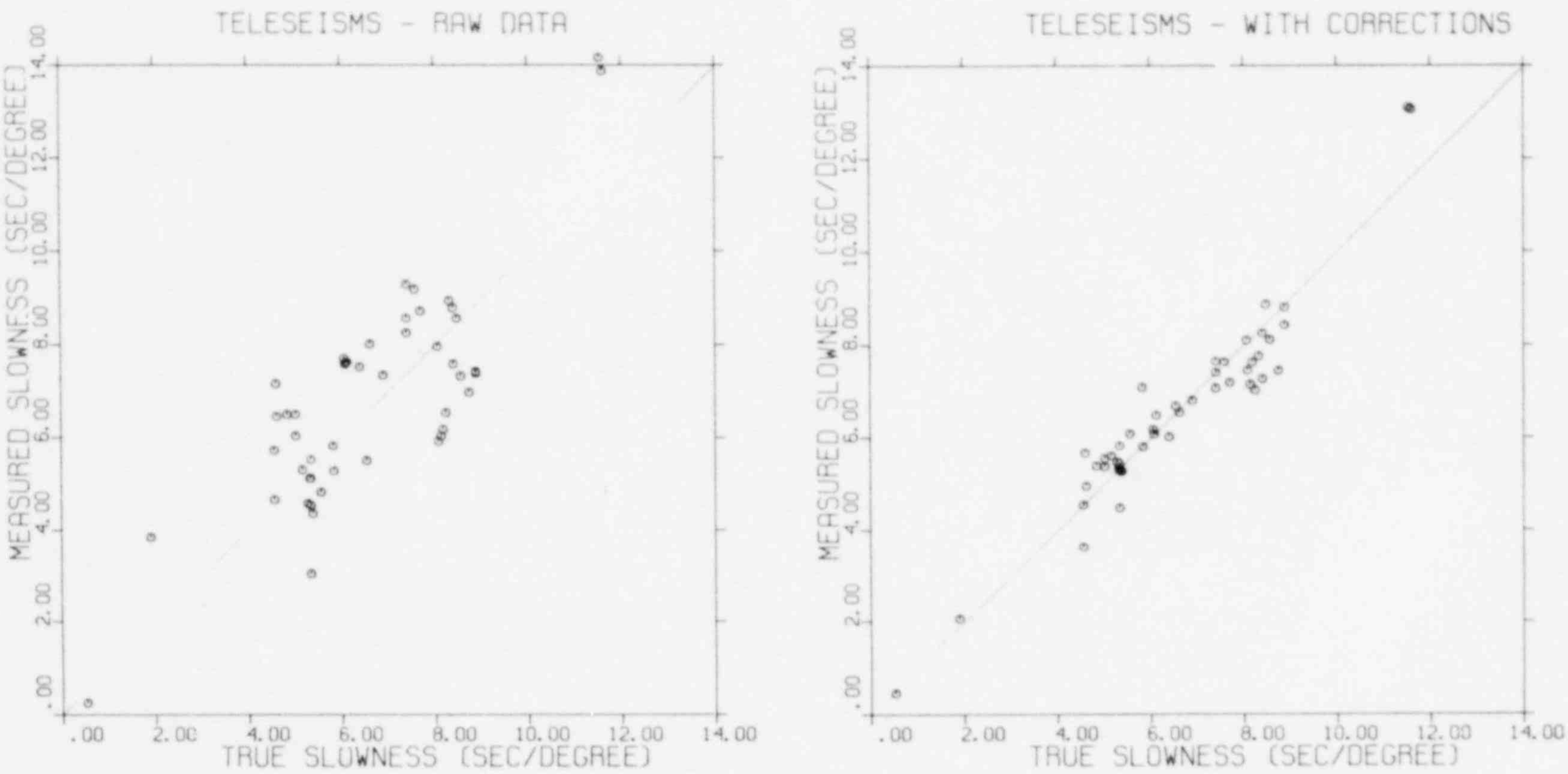

Figure 22: True vs Measured Apparent Horizontal Slowness, Before and After Applying Corrections Using Station Residuals

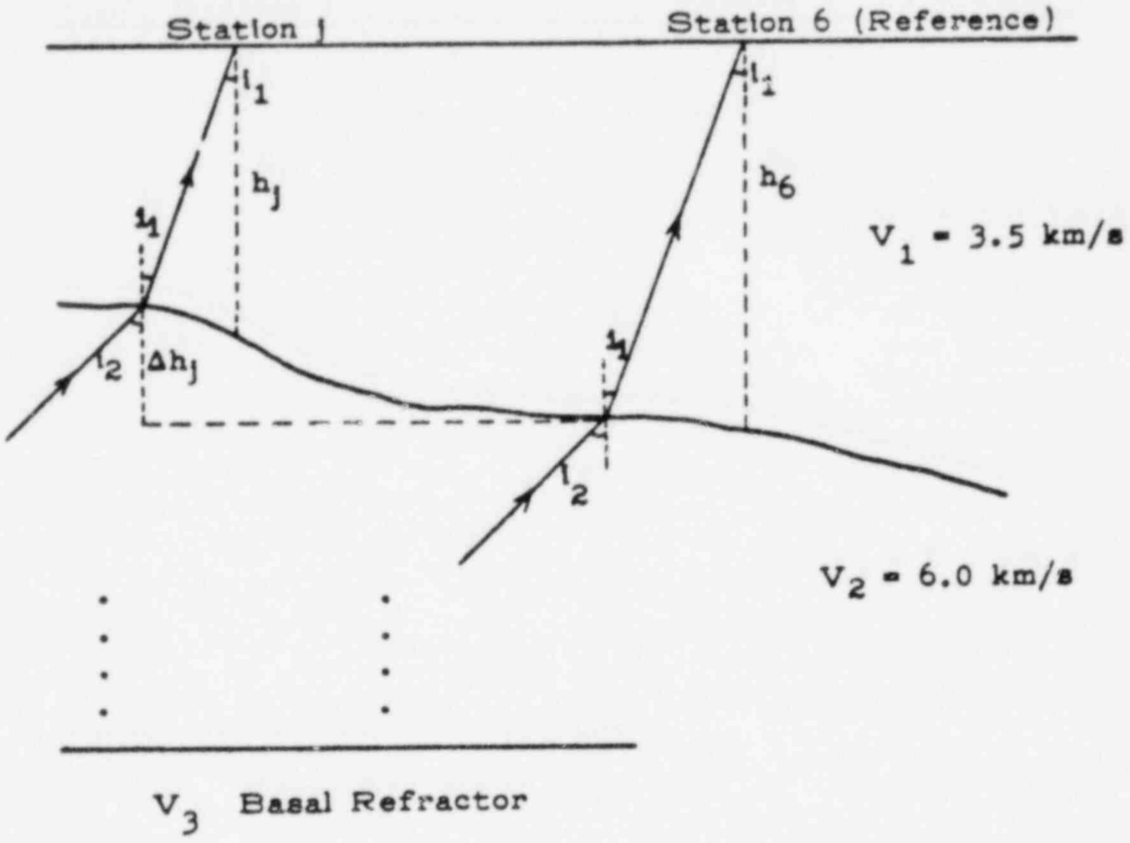

Near Surface Contribution to Station Residuals (secs)

Station j	h_j (Km)	Computed from Structure			Observed
		C $V_3 = \infty$	D $V_3 = 8$	E $V_3 = 7.2$	A
1	0.05	-.158	-.174	-.311	-.324 ∓ .166
2	1.21	-.019	-.021	-.037	-.058 ∓ .143
3	2.37	.119	.131	.235	.051 ∓ .126
4	2.20	.098	.108	.194	.180 ∓ .143
5	0.41	-.114	-.126	-.225	-.116 ∓ .099
6	1.37	0	0	0	0

Figure 23: Structure Model for Computing Expected Residuals, and a Comparison Between Expected and Observed Residuals Based Upon This Model

3) Hypocentral Location Techniques

A more detailed presentation of the following material will be found in Mosher (1980).

Our purpose here is to obtain accurate hypocentral locations for local and near-regional (to several hundred km) earthquakes. Our problem is somewhat unusual compared to conventional location techniques because (1) the epicenters lie outside of a small array rather than inside a large network, and (2) very few calibration earthquakes are available, although this limitation is compensated by the availability of many large mine blasts.

Data from the array for a particular event may be interpreted to yield (1) P and S travel times, if the origin time is known, (2) S-P time, if S can be identified, (3) azimuth of arrival, (4) apparent horizontal velocity for an equivalent plane wavefront, and (5) wavefront curvature. We have used this information to develop a multiple-step approach to obtaining hypocentral locations. These techniques, some of them new, have been especially designed for events which occur outside of the small array.

Azimuth to the event can be determined in a straightforward fashion from time moveouts across the array. Small corrections for array bias can be applied if necessary to yield correct azimuths to known events. The existence of wavefront curvature across the array, if any, does not invalidate the azimuth determinations.

In practise, we obtain the required observed values simultaneously for azimuth and apparent horizontal velocity by an iterative method based upon minimizing the sum of squares of residuals. The program includes an option to permit unequal variances in the observed arrival times.

A preliminary estimate of distance can be obtained from apparent horizontal velocity, which must equal the true velocity at the deepest point of the ray path in the absence of lateral velocity variations. A velocity model will be required to carry out this step. The velocity model can also be used to estimate distance using S-P times, if S can be identified on the waveform.

Total travel times and velocity-depth relationships can be obtained by integrating the apparent velocity data, subject to the usual non-uniqueness arising from possible velocity inversions. Mosher (1980) has reviewed the techniques by which to accomplish this and extended them to non-zero focal depths. From total travel times, Geiger's method can be used to locate hypocenters. Mosher (1980) has introduced modifications to Geiger's method to handle instabilities associated with events occurring outside of the array.

Our location method based upon wavefront curvature has the advantage that it requires minimal assumptions about the velocity structure, other than radial symmetry about the aperture of the event to the array. In particular, it will be independent of focal depth and independent of velocity variations with epicentral distance or depth. The geometry of this method is shown in Figure 24.

We have combined the travel time method (TTM) and the wavefront curvature method (WCM) into an iterative approach which will be referred to as Apparent Velocity Mapping (AVM). The steps in our process are as follows:

1. Compute epicenters using the WCM for those events located less than 3 array radii distant.

2. If mine blasts are available, compute apparent velocities using the WCM, constraining the epicenter to the known location.

3. Construct a zero-focus apparent velocity vs distance curve from the local earthquake and mine blast velocities. The curve should pass through the mine blast values and below the local earthquake values (assuming that velocity increases with depth).

4. Compute a velocity-depth function from the apparent velocity curve using the Herglotz-Wiechert integral.

5. Compute travel time tables from the velocity structure.

6. Recompute event hypocenters using the TTM. For distant events, focal depth may have to be constrained in order to obtain convergence. The depth can be constrained to a reasonable estimate so that an epicenter can be computed.

7. For those events for which focal depth was constrained, recompute focal depth using the method of apparent velocity deviations. If the recomputed focal depth is significantly different from the constrained value, the epicenter may have to be recomputed.

The above technique has been tested on synthetic data (based upon an assumed velocity model) and upon mine blast data whose locations and origin times are known. We find that the wavefront curvature method can be used satisfactorily only for events located less than 3 array radii distant, beyond which the emphasis must be shifted to the other components of the AVM method. The technique was used to locate the local earthquakes described in Section IV.

One final topic in connection with event location is removal of station bias. We have approached this by using a simplified version of the upper-crustal structure model obtained by Mooney et al (1970) and described in Section III.2. Our model is shown in Figure 25. The correction procedure can be summarized as follows:

1. Compute preliminary event locations using the AVM technique without corrections.

2. For a given event, calculate the distance x_j and azimuth ϕ_j of each station of the array to the event.

3. An apparent velocity table in terms of epicentral distance and focal depth will have been determined in step 1. The table may be used to compute ray parameter for each station:

$$P_j = 1 / V(x_j, h)$$

where V(x,h) is the apparent velocity table and h is focal depth of the event.

4. Convert the ray parameter for each station to an angle of incidence:

$$i_j = \sin^{-1}(p_j v_o)$$

where v_o is the surface velocity.

5. Use solid geometry to compute the path length d_j through the wedge for a ray from station j with azimuth $\emptyset_j$ and incident angle i_j.

6. Compute the correction Δt_j for each station using Equation 3-55. Subtract the corrections from the observed times to yield corrected times for the event.

7. Repeat steps 2 - 6 for each event.

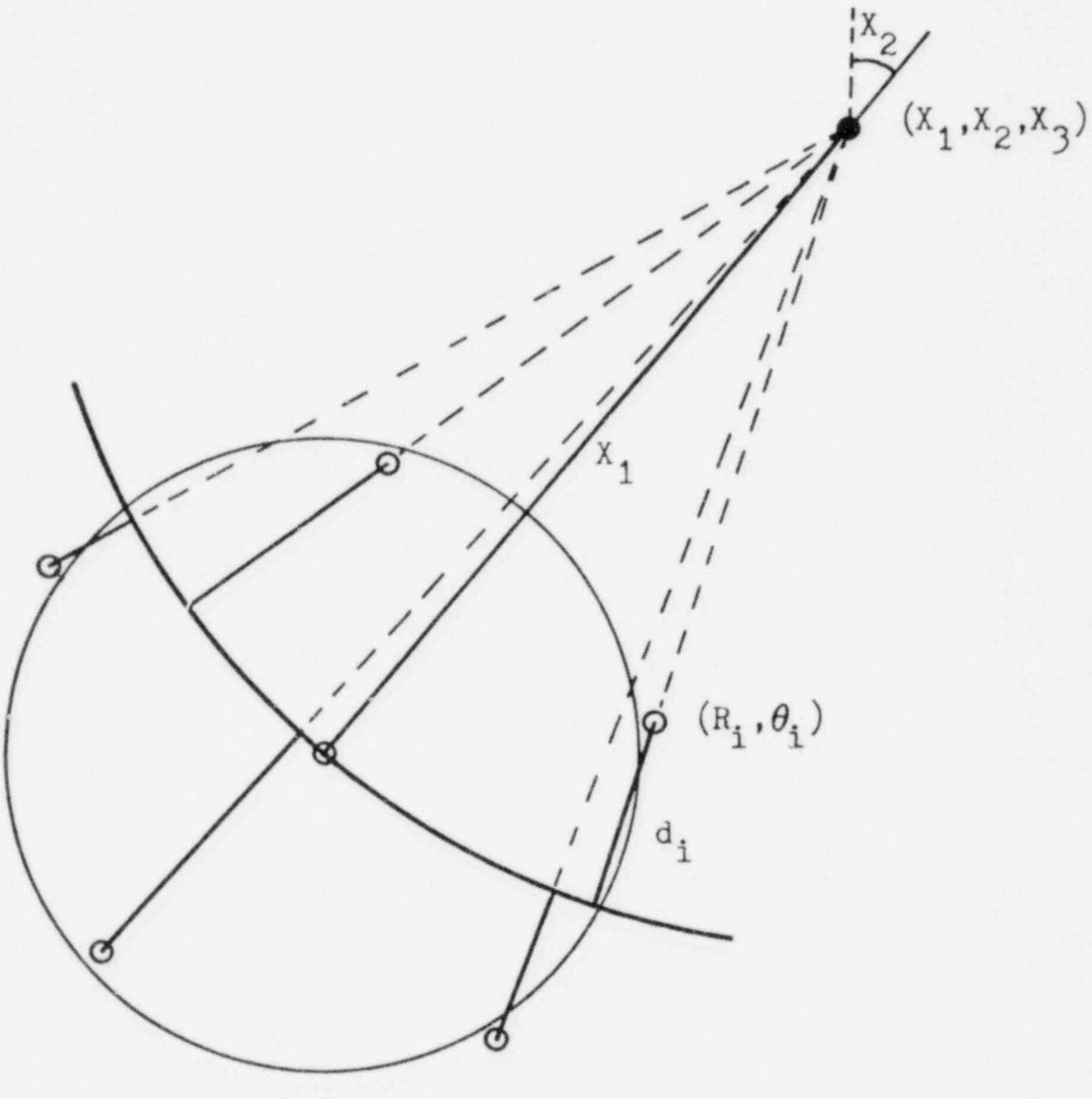

Figure 24: Theoretical Time Calculation for the Wavefront Curvature Method (WCM) of Location

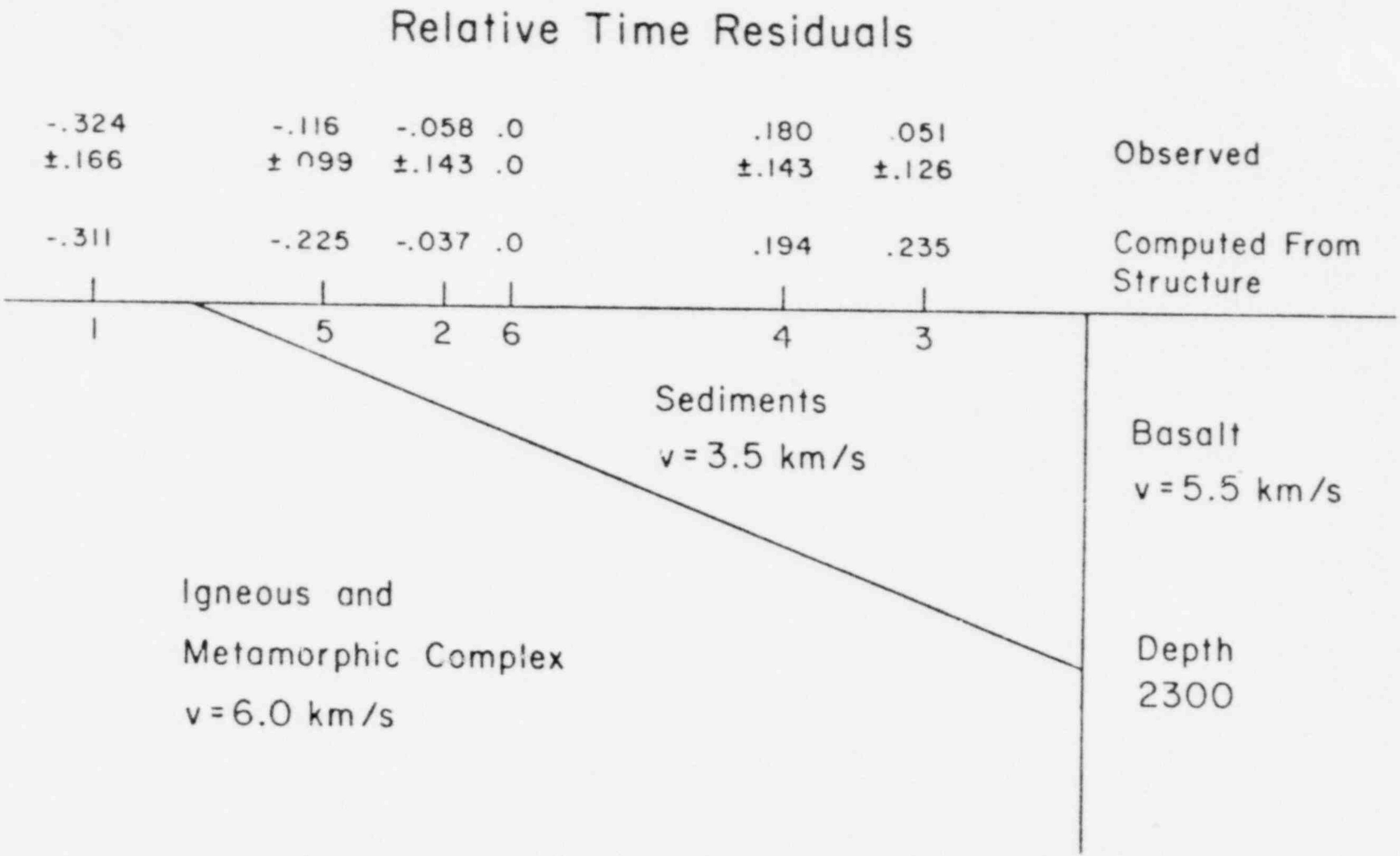

Figure 25: Structure Model Used for Computing Static Corrections

4) Magnitude Determinations for Local Earthquakes

A more detailed presentation of the following material will be found in Mosher (1980).

We have developed the local magnitude formula,

$$M_L = 2.57 \log\Delta + \log A - 3.97.$$

where Δ is in km and A is the maximum 1/2 peak to peak P wave ground displacement amplitude in 10^{-9} m for station CMSA-6.

The formula is derived by a combination of the following procedures and data sets: (1) The basic form of the equation used in Richter's (1935) original definition. (2) Relationship between seismic amplitude and charge size for known mine blasts, as obtained by Greenhalgh (1979). (3) A regional magnitude scale for the eastern United States based upon the amplitude of Pn, as developed by Evernden (1967). (4) Carpenter's (1967) predictions of teleseismic amplitudes of blasts in hard rock.

The above formula is intended for use with local and near-regional events near the Central Minnesota Seismic Array, for distances up to 300 km.

5) Refraction Seismic Profiles

A more detailed presentation of the following material will be found in Greenhalgh (1979).

Refraction seismic profiles can be used to obtain a velocity model for the region, thereby improving hypocenter determinations for local and regional earthquakes. A number of such profiles have been shot in the past within the Lake Superior geologic province. A review is presented by Greenhalgh (1979). The data set with most direct relevance to the present study was obtained by Mooney et al (1970).

Our contributions under the present contract consisted of three parts: (1) A 160-km profile extending from the Mesabi Iron Range (National Steel Company mine) to the CMSA, reported by Anderson (1978), (2) A more detailed 200-km profile extending from the Mesabi Iron Range (U.S. Steel Company mine) to the CMSA, currently under investigation by N. Wattrus, and (3) A composite travel time graph for the region derived by Greenhalgh (1979) based upon mine blast travel times plus apparent velocities across the array. Since Greenhalgh's analysis included data from the preceding two studies, we will present only his results here.

The first approach makes use of apparent velocities across the CMSA. The data are shown at the top of Figure 26. Subject to the approximation of two straight lines as shown, the time-distance curve can be obtained by integration to yield:

$$T = \frac{1}{a_1} \ln \frac{V_{o1} + a_1 X}{V_{o1}} \qquad 0 < X < X_c$$

$$T = \frac{1}{a_2} \ln \frac{V_{o2} + a_2 X}{V_c} + \frac{1}{a_1} \ln \frac{V_c}{V_{o1}} \qquad X_c < X < 230 \text{ km}$$

where $V_c = V_{o2} + a_2 X_c = V_{o1} + a_1 X_c$

$$X_c = \frac{V_{o1} - V_{o2}}{a_2 - a_1}$$

These expressions can be integrated by the Wiechert-Herglotz method to obtain velocity-depth functions. The results are presented in Table 4 and Figures 26 and 27.

The second approach is based upon a composite time-distance graph compiled by Greenhalgh (1979) from several sources. The result is shown in Figure 28. Three segments may be recognized:

1. The "direct wave" segment extending from X = 0-240 kms having apparent velocity of 6.0 - 6.5 km/s but increasing to 7.65 km/s at the larger distance ranges (X = 180-240 km).

2. The head wave (P_n) segment from X = 240-340 km having apparent velocity of 8.76 km/s. Note that the data points defining this segment are few and have only limited reliability i.e. the Morris and Minneapolis station times.

3. The reflection (P_mP) segment from X = 65-160 km having apparent velocity decreasing with X from 8.69 km/s to 6.99 km/s. and asymptotically approaching 6.0-6.5 km/s.

The other main feature of the T-X curve is the absence of first arrivals (direct wave segment) in the distance range X = 60-120 km.

Greenhalgh (1979) considered various possible interpretations for the preceding results. His preferred interpretation consists of

(1) Model B from Table 4 for the crust,

(2) Velocity discontinuity at the Moho,

(3) Moho depth = 42 km,

(4) Sub-Moho P velocity = 8.3 km/sec.

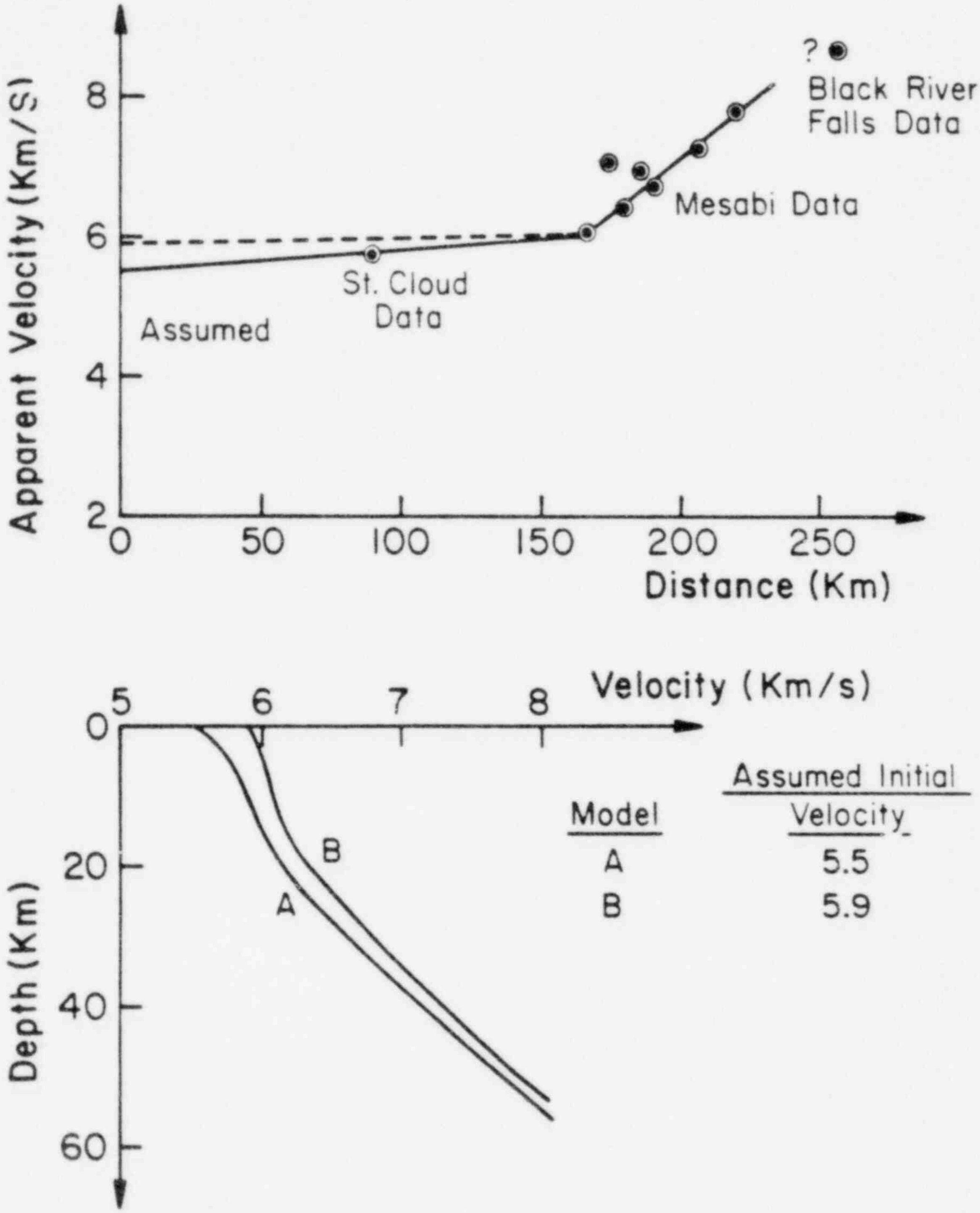

Figure 26: Observed Data for Apparent Velocities, and Two Inferred Velocity-Depth Functions

Table 4: V-X Models Used in V-Z Functions

Model		Velocity Parameters		
		V_{o1} km/s	X_c (km)	V_c (km/s)
A	Line II a_2 = .03264 s^{-1} V_{o2} = .561 km/s	5.5	154.5	6.0
B		5.9	154.5	6.0
C	Line I a_2 = .02616 s^{-1} V_{o2} = 1.96 km/s	5.5	154.5	6.0
D		5.9	154.5	6.0
E		5.5	164	6.25
F		5.9	164	6.25

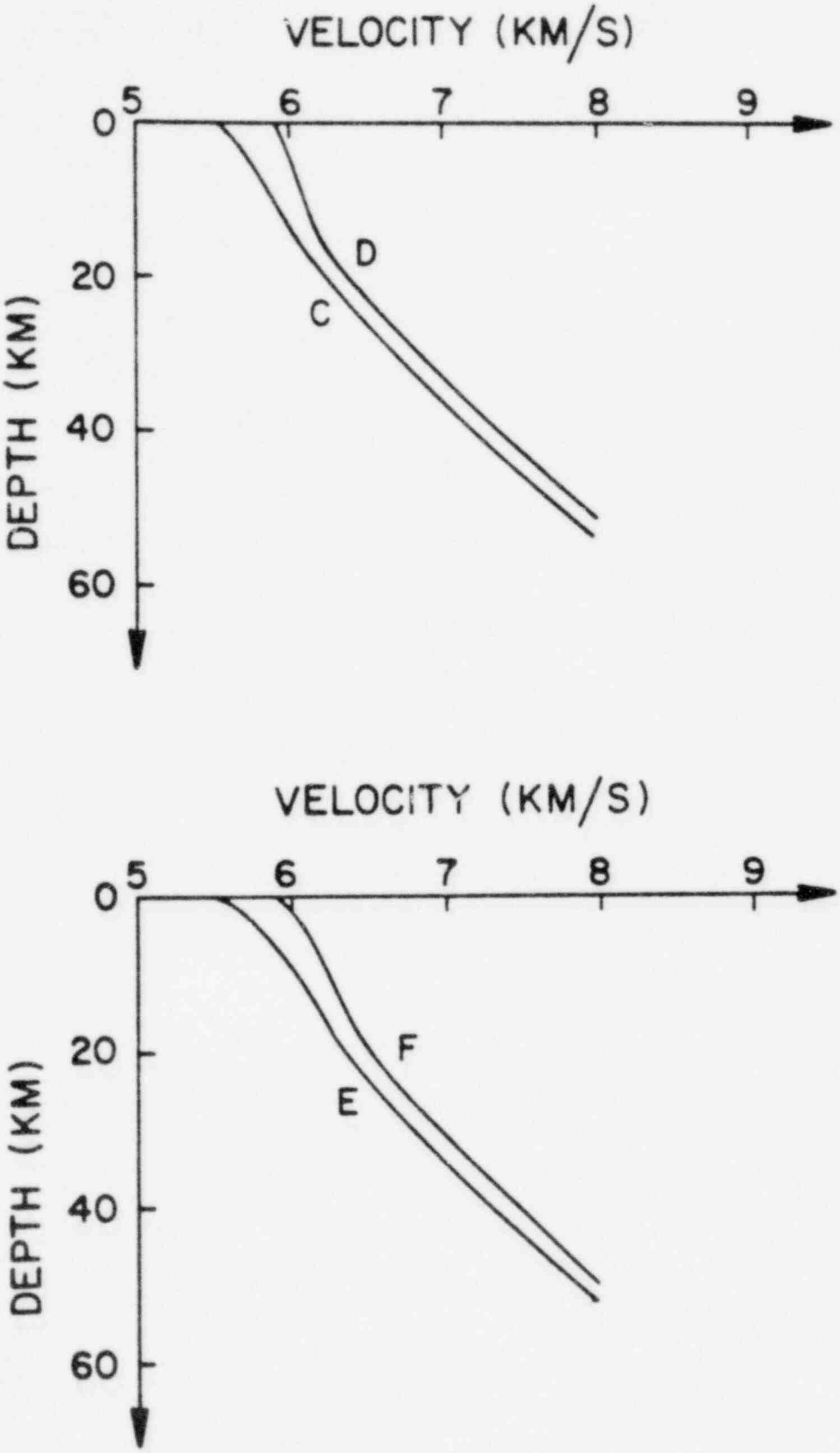

Figure 27: Inferred Velocity-Depth Functions Based upon Parameters of Table 4

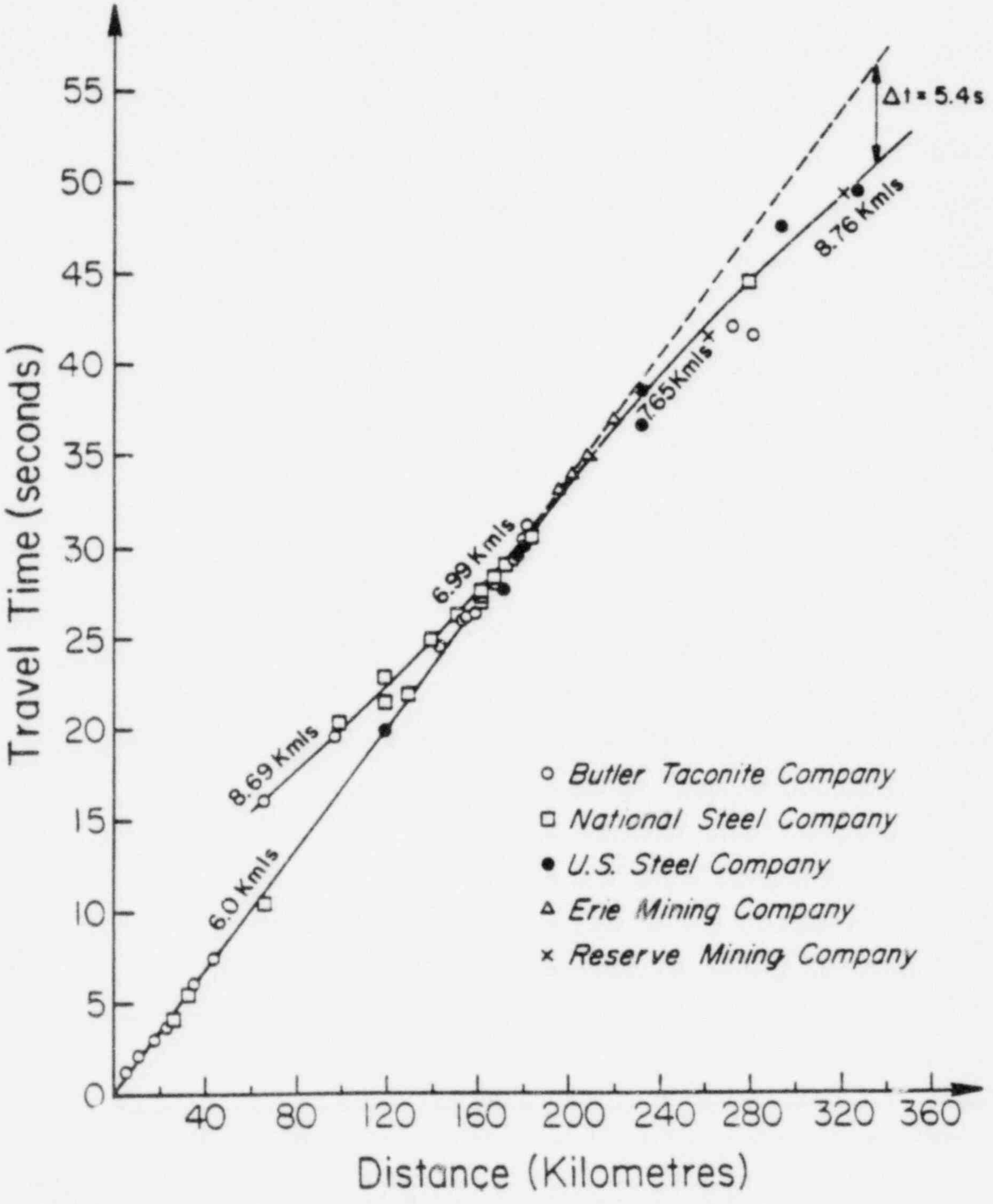

Figure 28: Composite Time-Distance Graph for Mesabi Mine Blasts

6) Surface wave studies

A more detailed presentation of the following material will be found in Mosher (1980).

Strong surface wave trains are observed from some (but not all) Mesabi Iron Range blasts. Analysis of these surface waves has the potential to provide stronger constraints on the regional velocity distribution, especially with respect to shear wave velocities. An improved velocity distribution would, in turn, lead to improved location capabilities for local and regional earthquakes.

Figure 29 shows a representative surface wave train from a Mesabi mine blast. A notable feature is the presence of two distinct wave trains, most clearly at station CM6, which we have designated R1 and R2. Detailed analysis has shown that these waves not only arrive with different apparent velocities but also from different azimuths, and that R1 is made up of two separate overlapping signals. We have supplementary data (not shown here) from three-component recordings which support the interpretation that the wave motion is of Rayleigh type.

Our analysis of these signals proceeded in several stages. We first computed group velocities by the standard peak and trough technique. We next applied a modification of the multiple filter analysis method originated by Dziewsonski, Bloch, and Landisman (1969). This was then combined with complex trace analysis to yield two modes of output display: an envelope stack showing frequency vs time, and a matrix display of amplitudes contoured on a frequency-time grid. Illustrations of these results are shown in Figures 30, 31 and 32. The distinction between R1 and R2, and the subdivision within R1, can be clearly seen in Figure 32.

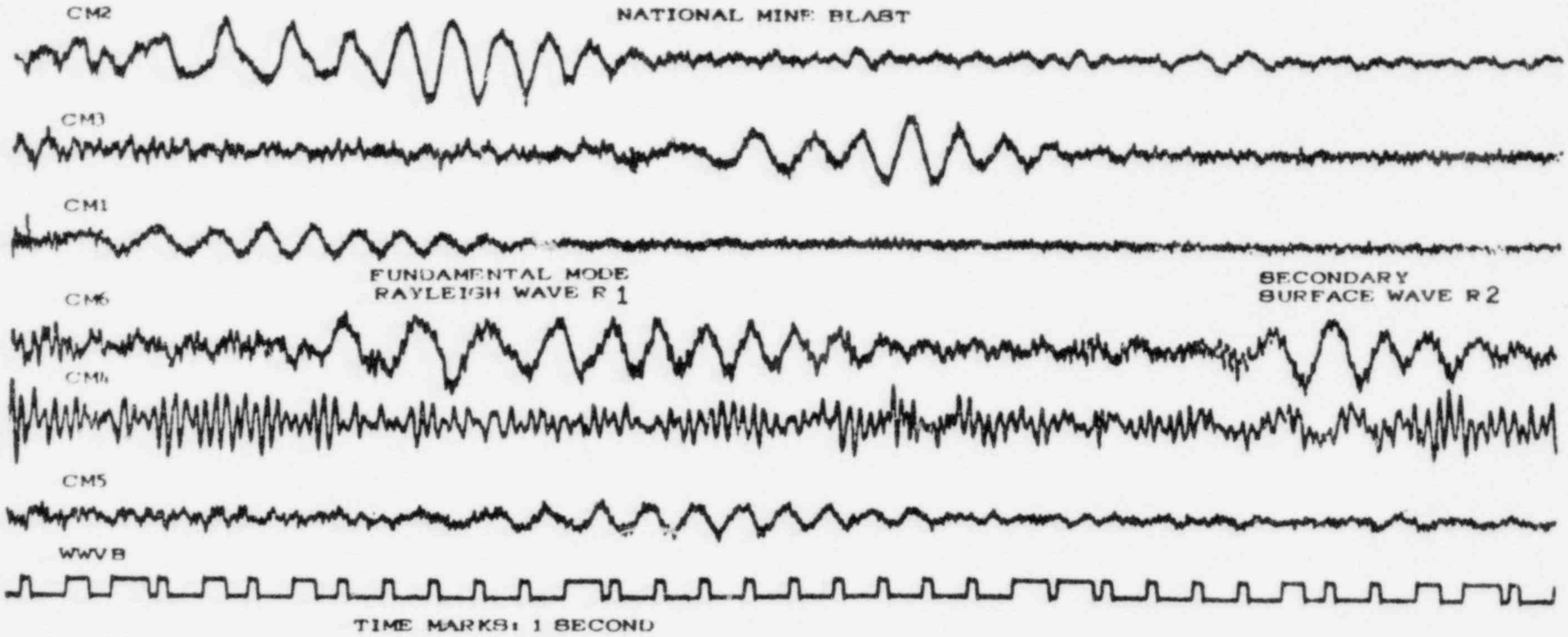

Figure 29: Representative Surface Wave Train as Recorded at CMSA from Mesabi Mine Blast

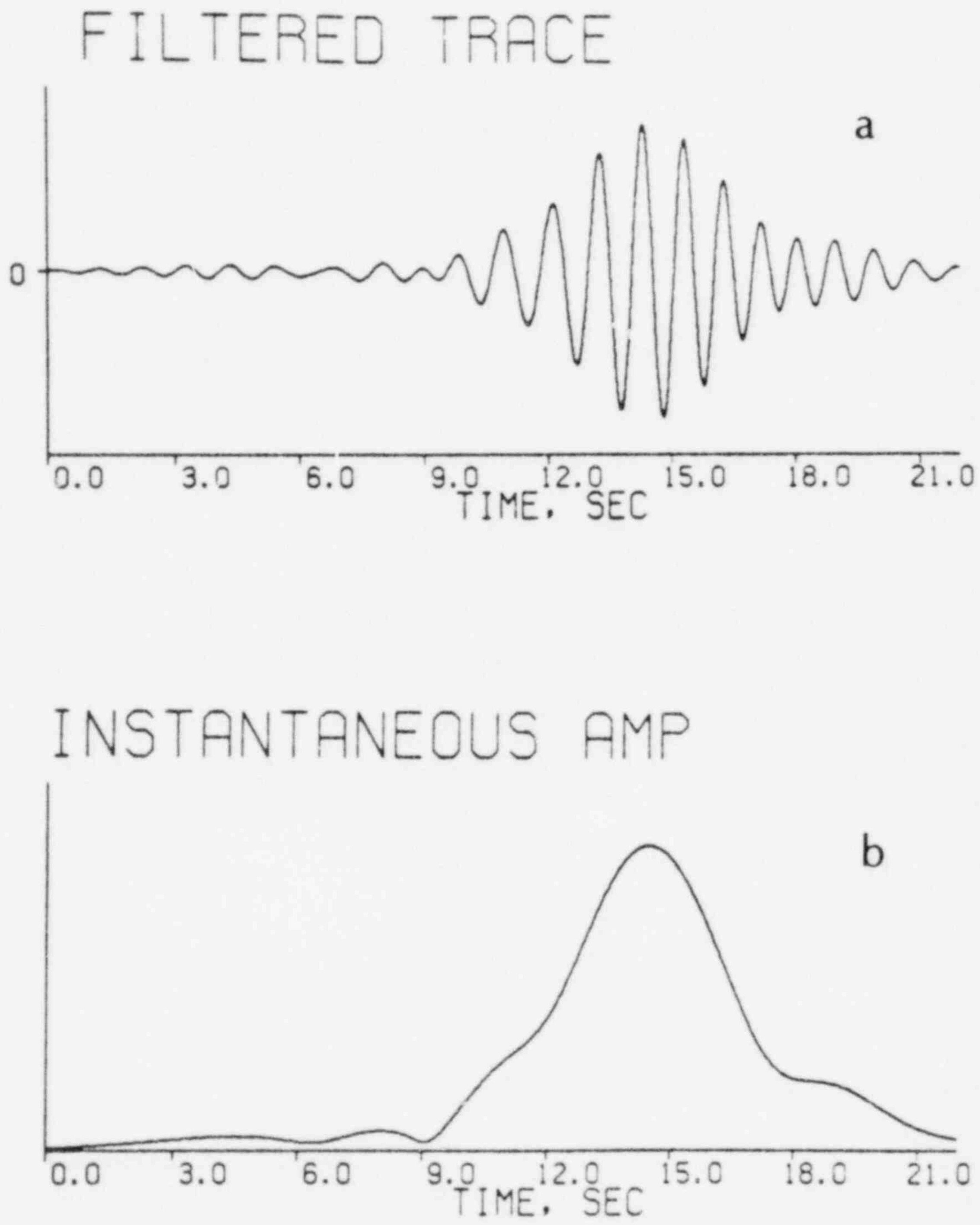

Figure 30: Illustration of Complex Trace Analysis. Top Trace Shows Surface Wave Train Band-Pass Filtered at 1 Hz. Lower Trace Shows Instaneous Amplitude of Complex Trace.

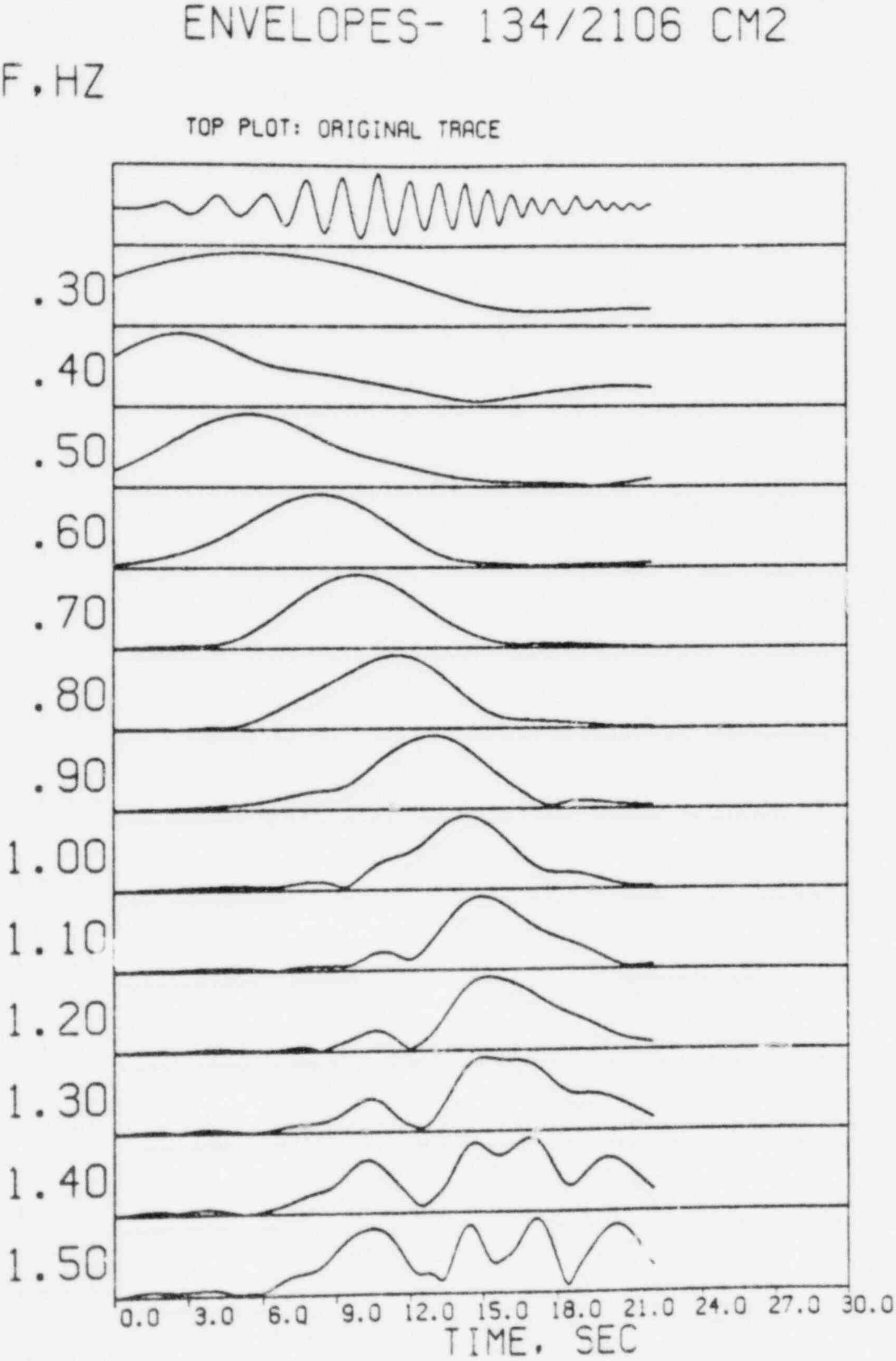

Figure 31: Envelope Stack for Complex Trace Amplitude, Showing Frequency vs Arrival Time

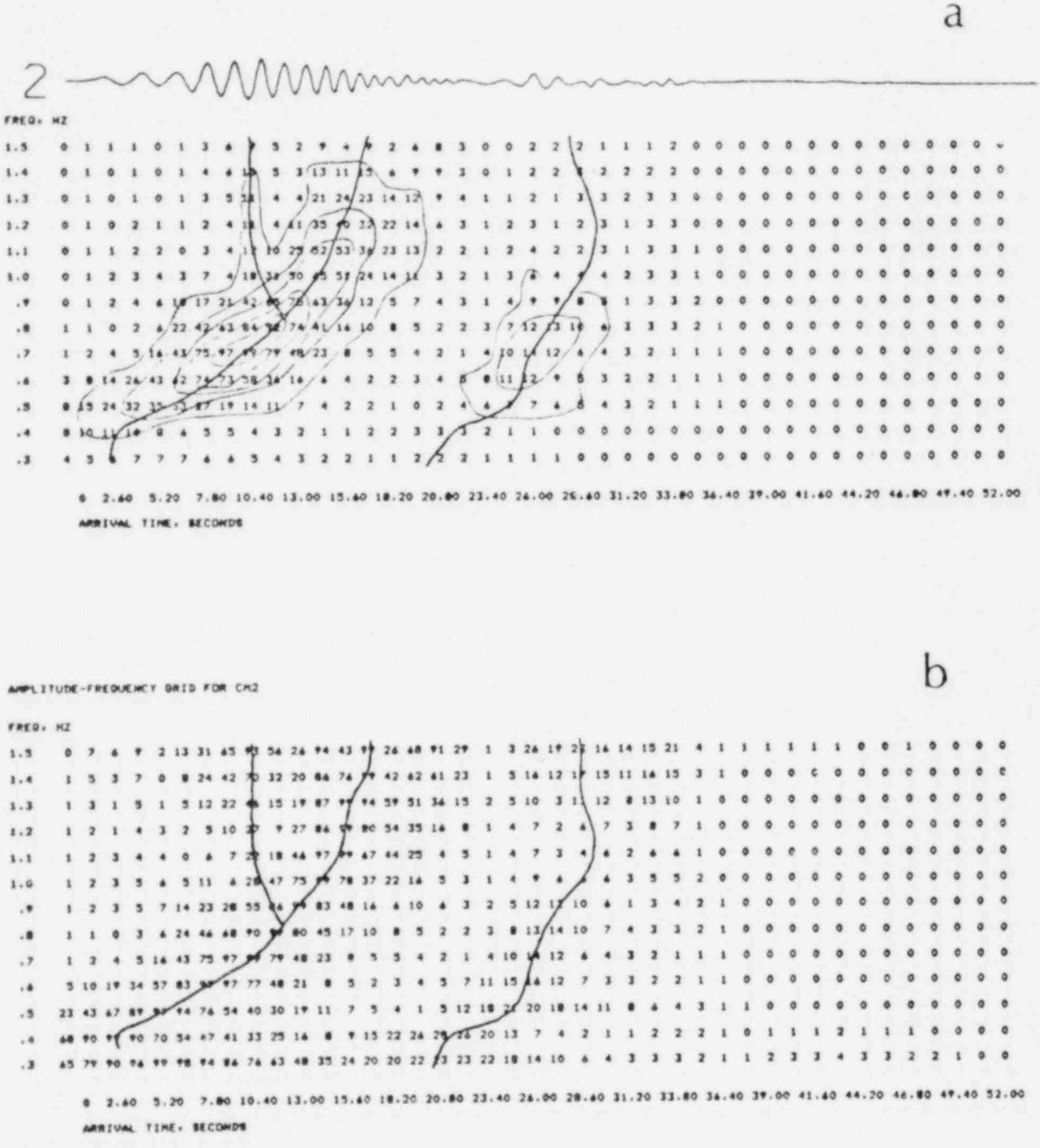

Figure 32: Multiple Filter Analysis Amplitude Grids for Waveform at Top (Lower Grid is Row Normalized)

We carried out many analyses of this sort. Table 5 displays some of the results for the R1 arrival. The lower two boxes show the distinction between array stations overlying the shallower portions of the sedimentary wedge and those overlying the deeper portions. One of the most striking conclusions from Table 5 is the departure of the observed arrival azimuth from the known azimuth to the mines. The former is nearly constant, despite a range of 26° in true azimuths. We interpret these results to indicate lateral refraction by the sedimentary wedge. The refraction effect is also frequency dependent, as may be seen in Figure 33.

Results for the R1 arrival may be summarized as follows:

1. Observed azimuths of surface waves deviate considerably from the azimuths to the known sources. The largest part of the azimuth deviation is due to the refracting effect of the wedge of low velocity sediments located beneath the CMSA. A smaller portion of the deviation may be due to refraction that occurs in the Animikie Group, a slightly dipping series of metasediments located to the north of the CMSA.

2. Observed phase velocities for an array subset located on the shallow side of the wedge of low velocity sediments are higher than those observed for a subset on the deep side of the wedge. The shallow values decrease from 2.5 km/s at .4 Hz to 1.7 km/s at 1.5 Hz. The observed phase velocities for the deep subset are relatively constant, at 1.4 km/s. These velocities are consistent with those calculated from the three layer model for the wedge.

3. Observed surface wave dispersion is normal for propagation across the shallow half of the wedge. This means that high frequencies are delayed in time relative to low frequencies. For propagation across the deep half of the wedge, surface wave dispersion is reverse: high frequencies are advanced in time relative to lower frequencies. The observations of surface wave dispersion are consistent with group velocity curves computed for the model. Surface wave amplitudes are also consistent with the model.

Table 5: Summary of Surface Wave Analyses
for Mesabi Mine Blasts

R1 CM1-6

Event	Mine	f range (Hz)	$\bar{V}_p$	$\overline{Az}$	True Az
134/2106	Reserve	.5 - 1.2	1.76+-.04	318.6+-1.6	25.0
135/2114	US Steel	.3 - 1.3	1.53+-.07	328.6+-2.8	12.5
138/0804	National	.4 - 1.1	1.76+-.09	314.7+-3.2	3.45
139/2188	Butler	.4 - 1.0	2.02+-.18	336.2+-5.4	359.3
142/1409	Eveleth	.5 - 1.2	1.93+-.12	313.1+-4.0	15.3

Ave V_p = 1.73+-.03

R1 CM1256 (Shallow)

108/1476	Erie	.4 - 1.2	1.76+-.39	323.9+-12.	22.5
134/2106	Reserve	.5 - 1.2	1.71+-.01	320.9+-.11	25.0
135/2114	US Steel	.3 - 1.3	2.05+-.04	333.7+-1.1	12.5
139/2188	Butler	.5 - 1.1	1.68 +.01	322.1+-.30	359.3
142/1409	Eveleth	.5 - 1.2	1.81+-.06	319.6+-1.9	15.3

Ave V_p = 1.71+-.01

R1 CM2346 (Deep)

134/2106	Reserve	.5 - 1.2	1.53+-.02	319.1+-.7	25.0
135/2114	US Steel	.3 - 1.3	1.39+-.01	318.5+-.5	12.5
142/1409	Eveleth	.5 - 1.2	1.43+-.02	278.5+-.7	15.3

Ave V_p = 1.42+-.01

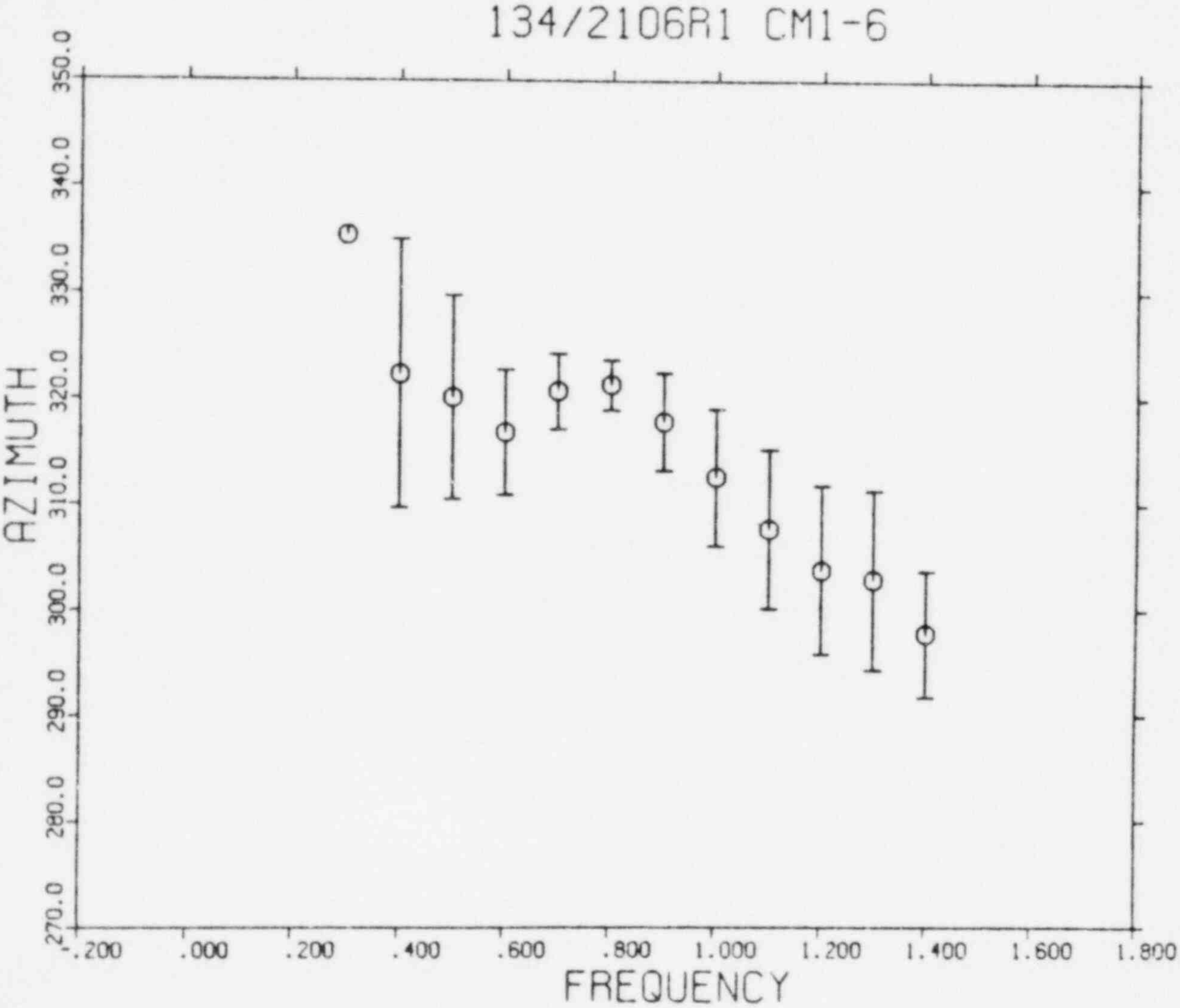

Figure 33: Dependence of Azimuth of Arrival Upon Frequency, for Surface Wave Train

Our interpretation of the various kinds of analysis applied to surface waves may be summarized as follows: R1 is considered to be the fundamental Rayleigh mode on the basis of phase velocity (ave. 1.7 km/s) and preliminary analysis of three component records. The variation of R1 phase velocity across the array was investigated by performing computations using array subsets located over different parts of the sedimentary wedge beneath the array. A model approximating the wedge structure was constructed from the refraction profiles of Mooney et al, (1970). Phase velocities were found to be consistent with this model. The change in observed dispersion and relative surface wave amplitude was also consistent with the model.

Considerable lateral refraction of R1 was revealed in the azimuth vs frequency curves. A large part of the observed refraction can be explained by the change in phase velocity as the sedimentary wedge beneath the array thickens. The remainder of the observed refraction must be assigned to an earlier portion of the travel path.

Azimuth of the R2 arrival differs considerably from that of R1. Whereas R1 appears to arrive from the northwest, R2 appears to arrive from the northeast. The most likely origin for R2 is a reflection from the Douglas Fault to the northeast of the array. The Douglas Fault forms the western boundary of the St. Croix Horst. Models approximating the structure of the wedge and fault indicate that if a reflection occurs, it must be partial. Calculations of the energy in R1 and R2 confirm a partial reflection. Phase velocities for R2 (ave. 1.0 km/s) are lower than R1 velocities.

The R1′ arrival appears to be a higher mode Rayleigh wave generated along an earlier portion of the travel path. All higher modes are cut off for reasonable wedge models, so Rl' should travel at the same velocity as Rl across the wedge. Observed phase velocities for Rl' (average 1.9 km/s) are higher than velocities for Rl. The discrepancy is small enough to be accounted for by the errors in the observations. Rl' is probably generated in the Animikie Group, a series of metasediments located north of the CMSA.

IV. Seismicity Studies and Seismicity Results

1) Local Earthquakes Detected by the Central Minnesota Seismic Array

Three local earthquakes have been observed to date during operation of the Central Minnesota Seismic Array. Their relationship to regional tectonics will be considered in the following section.

The CMSA records for the three events are shown in Figures 34, 35, and 36.

Parameters for the events are presented in Table 6. The epicentral locations and magnitude determinations were obtained following procedures described in Section III.

We wish to address one question which will naturally occur to the reader. The three events which we report occurred within a three-month period in 1979, wheras no events occurred during the previous two years. Is it possible that detection capability for the array or identification capability of the interpreters improved markedly in early 1979?

We contend that both of the above factors remained approximately equivalent during the operating period of the array. As noted earlier, every recorded event has been played back and studied. This includes hundreds of teleseisms and hundreds of mine blasts. Seismic waveforms for teleseisms and regional earthquakes are so different from the local earthquakes that no misinterpretation is possible. The Mesabi mine blasts are repetitive in waveform and characteristic in azimuth of arrival, so much so that we find it possible to distinguish one mine from another. Several other mines and quarries (Marquette Iron Range in Michigan; Black River Falls, Wisconsin; Dresser, Wisconsin; Atikohan, Ontario) produce distinctive waveforms, azimuths of arrival, and sequence of body and surface waves. In addition to these characteristics, all of the blasts occur in a narrow time window, mostly between 11:00 A.M. and 3:00 P.M. local time.

We have reviewed our instrument sensitivities and our identification and interpretation procedures for the three years of array operation. We find no significant change. The hundreds of identified events have been recorded at comparable levels and have received comparable interpretations over the three years.

We conclude that the "burst" of seismic activity in early 1979 is real.

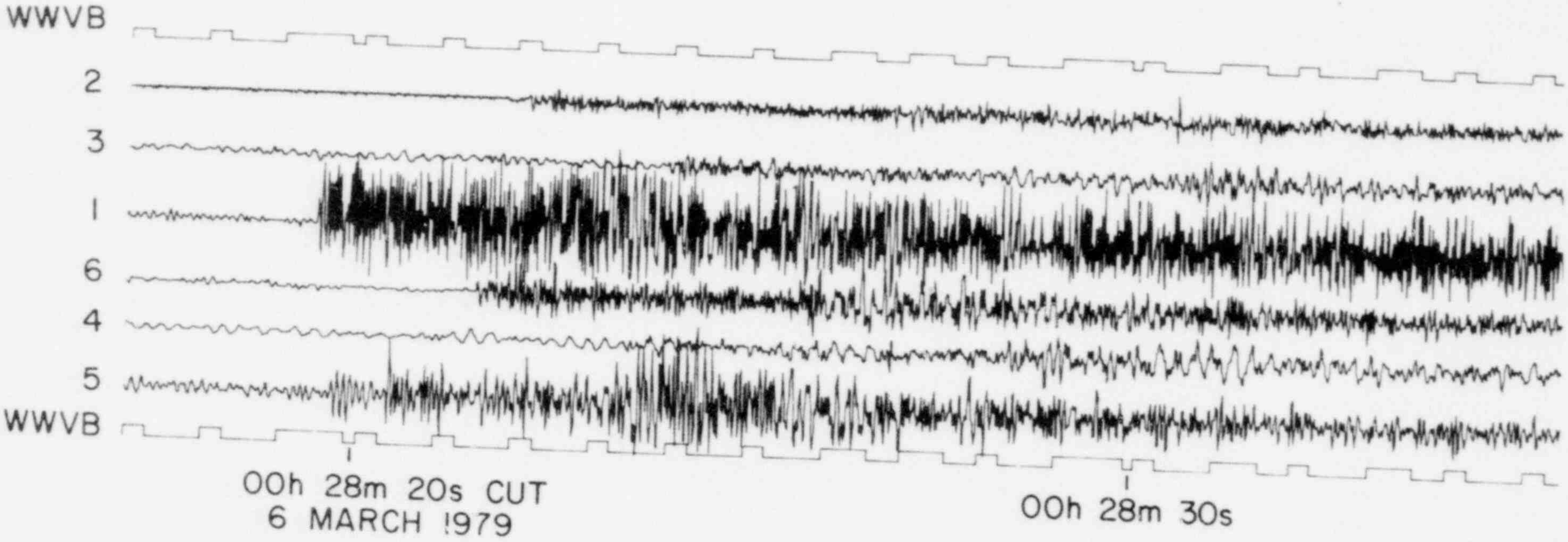

Figure 34: CMSA Record for Minnesota Earthquake of 6 March, 1979

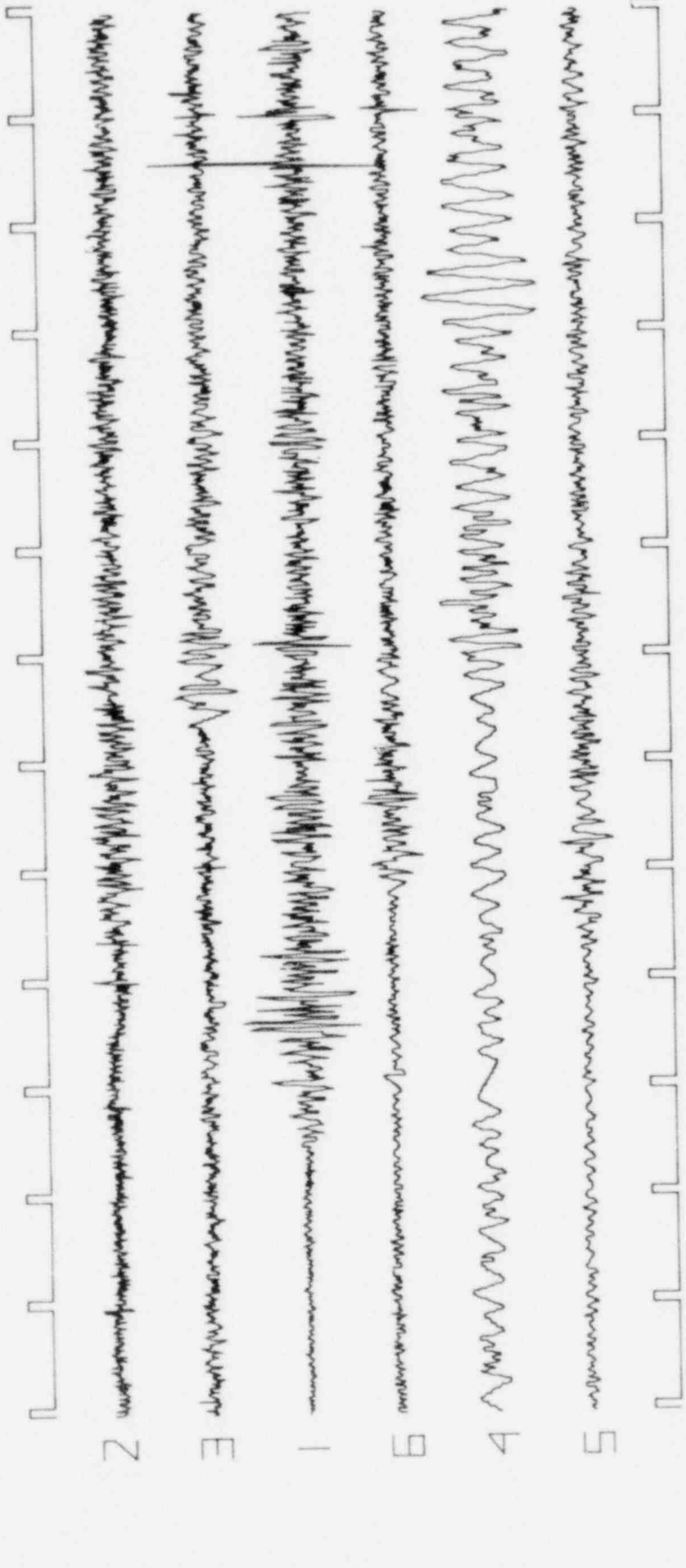

Figure 35: CMSA Record for Minnesota Earthquake of 16 April, 1979

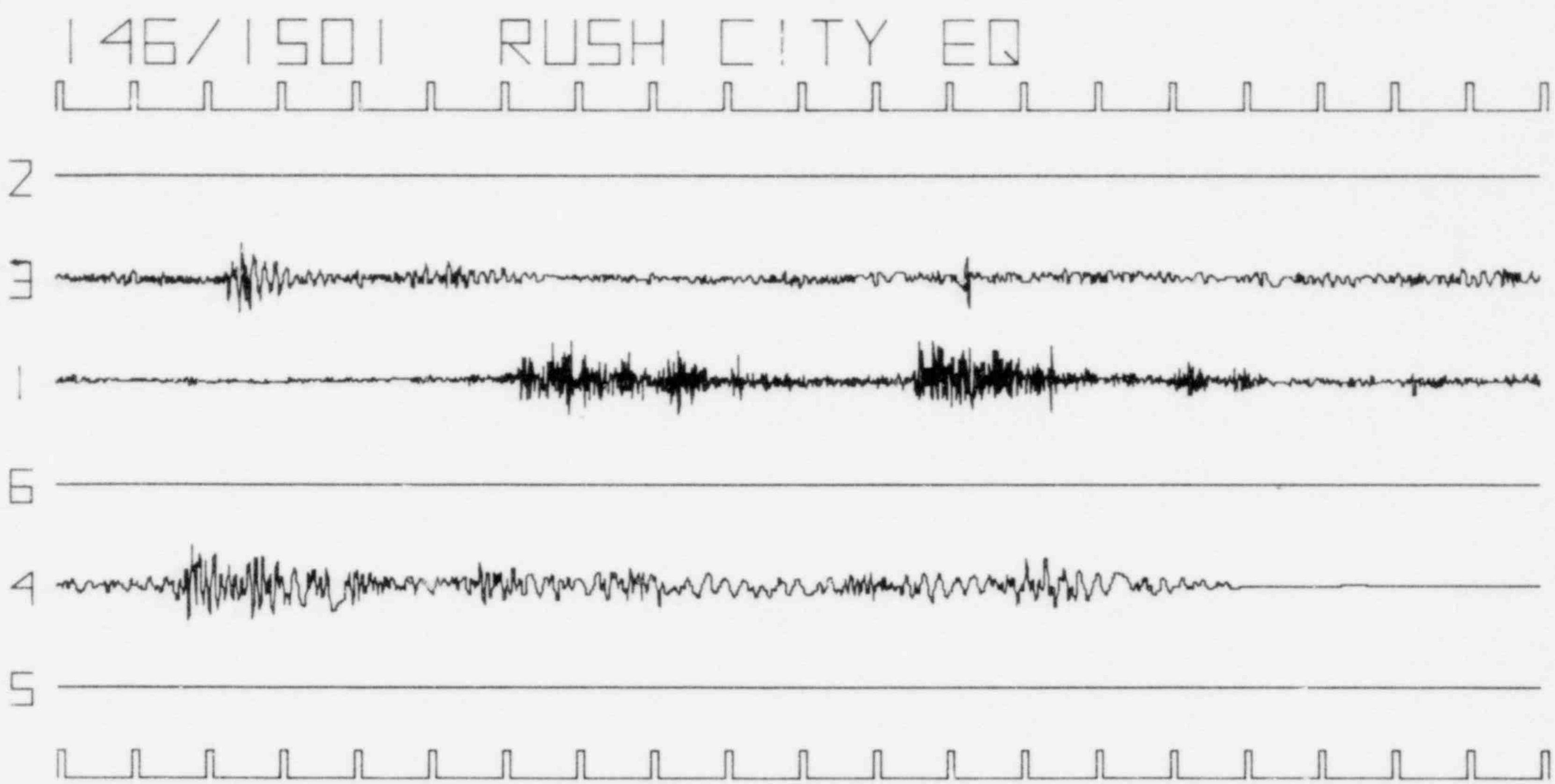

Figure 36: CMSA Record for Minnesota Earthquake of 14 May, 1979

Table 6: Parameters for Local Earthquakes Recorded by the Central Minnesota Seismic Array

Date	6 March 1979	16 April 1979	14 May 1979
Origin time	00h27m56.1s CUT	6h40m16.7s CUT	19h27m38.5s CUT
North Latitude	45°50'51"	46°41'48"	45°43'12"
West Longitude	93°44'53"	95°32'24"	92°59'31"
Depth	5 km	20 km	6 km
Magnitude	1.0	3.1	0.1
Location	Milaca, MN	Detroit Lakes, MN	Rush City, MN
Distance from CMSA-6	42 km	208 km	22 km
Azimuth from CMSA-6	268°	300°	134°

2) Historical seismicity and tectonic relationships

A more detailed presentation of the following material will be found in Mooney (1979) and Mooney and Morey (1980).

Table 7 presents a listing of all known earthquakes with epicenters within Minnesota, including the three events described in the previous section. The references cited above discuss such questions as methods to assign magnitude, uncertainties in epicentral locations, etc. Figure 37 shows the locations of these epicenters superposed on a new tectonic map of the state.

The epicenters show a clear relationship to tectonic features of the state. Four epicenters lie along the newly defined Great Lakes Tectonic Zone, an east-northeast-trending belt extending across several states and into Canada. The zone separates 3,000 - 3,600 m.y. rocks of a gneissic terrane to the south from 2,700 m.y. rocks of a greenstone-granite terrane to the north. Four other events lie on known major northwest-trending faults in the greenstone-granite terrane. Two and possibly three events are associated with the western margin of the Midcontinent Rift System.

Table 7: Parameters of Minnesota Earthquakes (from Mooney and Morey, 1980)

	Location	Date	Time (CUT)	Latitude (north)	Longitude (west)	Felt Area (km^2)	Intensity (MM, max)	Magnitude
1.	Long Prairie	1860-61		46°06.0'	94°52.0'		VI-VII	4.6
2.	New Prague	1860, Dec 16	18h	44°32.8'	93°31.4'		VI	4.3
3.	Red Lake	1917, Feb 6	17h26m	47°55'	95°00'			
4.	Staples (Motley)	1917, Sep 3	21h30m	46°20.2'	94°38.0'	48,000	VI-VII	4.8
5.	Bowstring	1928, Dec 23	06h10m	47°32.5'	93°47.6'		III	3.1
6.	Detroit Lakes (Audubon)	1939, Jan 28	17h55m	46°52.0'	95°59.0'	8,000	IV	3.7
7.	Alexandria	1950, Feb 15	04h05m	45°58'	95°22'		V-VII	3.8
8.	Pipestone	1964, Sep 28		44.0°	96.4°			3.4
9.	Morris	1975, Jul 9	14h54m15.1s	45°39.0'	96°05.0'	82,000	VI	4.6
10.	Milaca	1979, Mar 6	00h27m56.1s	45°50.8'	93°44.9'			1.0
11.	Evergreen	1979, Apr 16	06h40m16.7s	46°46.8'	95°32.8'			3.1
12.	Rush City	1979, May 14	19h27m38.5s	45°43.2'	92°59.5'			0.1

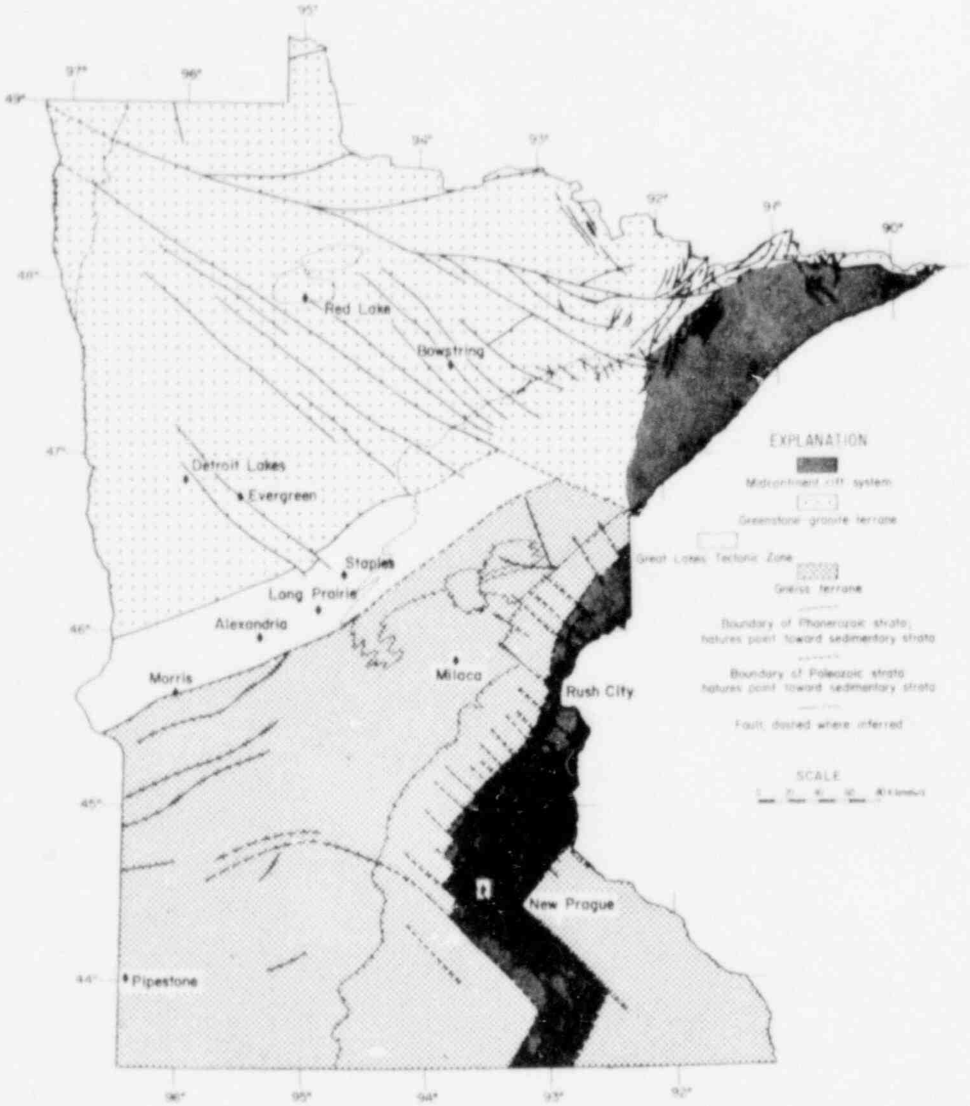

Figure 37: Historical Seismicity of Minnesota and Its Relationship to Regional Geology (from Mooney and Morey, 1980)

REFERENCES (Other Than Those Listed in Appendix A)

Mooney, H.M., C. Craddock, P. R. Farnham, S.H. Johnson, and G. Volz, 1970, Refraction Seismic Investigations of the Northern Midcontinent Gravity High: Jour. Geophysical Research, v. 75, p. 5056-5086.

Mooney, H.M., P.R. Farnham, S.H. Johnson, G. Volz, and C. Craddock, 1970, Seismic Studies over the Midcontinent Gravity High in Minnesota and Northwestern Wisconsin: Report of Investigations 11, Minnesota Geological Survey, 191 pp.

Sims, P.K., Carel, K.D., Morey, G.B. and Peterman, Z.E., 1980, The Great Lakes Tectonic Zone--a major Precambrian crustal structure in central North America: Geological Society of America, Bulletin (to be published in late 1980).

APPENDIX A: Bibliography of Publications and Reports Prepared under Contract NRC-04-76-289*

1 August, 1977	Seismic Event Log, CMSA, January-March, 1977
1 August, 1977	Seismic Event Log, CMSA, April-June, 1977
1 October, 1977	Annual Report, 1 October, 1976, to 30 September, 1977
1 November, 1977	Seismic Event Log, CMSA, July-September, 1977
24 December, 1977	Technical Report TR 1977-1: Note on the "Chicago Event" of 18 November, 1977, as recorded on Central Minnesota Seismic Array. 3 pp.
15 July, 1978	Seismic Event Log, CMSA, October-December, 1977
15 July, 1978	Seismic Event Log, CMSA, January-March, 1978
15 July, 1978	Technical Report TR 1978-4: System Documentation for Central Minnesota Seismic Array and Affiliated Stations, 23 pp.
1 August, 1978	Seismic Event Log, CMSA, April-June, 1978
15 August, 1978	Technical Report TR 1978-3: Crustal Structure Calibration for the Central Minnesota Seismic Array -- A 160-km Crustal Refraction Profile
15 August, 1978	Technical Report TR 1978-2: A Study of Mine Blasts for Magnitude Calibration for the Central Minnesota Seismic Array
15 August, 1978	Cumulative Bibliography, of Reports Submitted under Contract NRC-04-76-289, Version 197 Version 1978-1
15 August, 1978	Technical Report TR 1978-1: A Study of Array Bias and Its Removal for the Central Minnesota Seismic Array , 30 pp.
15 September, 1978	Cumulative List of Oral Presentations at Meetings in Connection with Contract NRC-04-76-289, Version 1978-1.

*Available in the NRC Public Document Room for inspection and copying for a fee.

Appendix A (continued)

1 October, 1978	Annual Report, 1 October, 1977 to 30 September, 1978
	M.S. Thesis, University of Minnesota. Anderson, R. A., 1978, Northern Minnesota Seismic Refraction Profile: 129 pp.
1 January, 1979	Quarterly Report.
1 February, 1979	Revised Comprehensive Seismic Event Log, Central Minnesota Seismic Array, 20 December, 1976, to 30 June, 1977, 21 pages.
	Ibid, 1 July, 1977, to 31 December, 1977, 19 pages.
	Ibid 1 January, 1978, to 31 March, 1978, 27 pages.
	Ibid 1 April, 1978, to 30 June, 1978, 30 pages.
	Ibid 1 July, 1978, to 30 September, 1978, 17 pages.
1 April, 1979	Quarterly Report.
15 May, 1979	Ph.D. Thesis, University of Minnesota.
	Greenhalgh, S.A., 1979, Studies with a Small Array in East-Central Minnesota: xxx + 323 pp.
1 June, 1979	Technical Report 1979-1: A Study of Array Bias (Revised), 18 pp.
15 June, 1979	M.S. Thesis, University of Minnesota.
	Mosher, C.C., 1979, Magnitude Calibration for the Central Minnesota Seismic Array: 92 pp.
25 June, 1979	Technical Report 1979-2: The Central Minnesota Earthquake of 5 March, 1979, 6 pp.
1 July, 1979	Annual Report.
1 October, 1979	Quarterly Report.
17 October, 1979	Technical Report 1979-3: The Central Minnesota Earthquake of 16 April, 1979, pp.

Appendix A (continued)

20 October, 1979	"Earthquake History of Minnesota" by Harold M. Mooney. Report of Investigations 23, Minnesota Geological Survey, 1633 North Eustis, St. Paul MN 55108, 20 pp
15 November, 1979	Technical Report 1979-4: Seismic Event Log for Central Minnesota Seismic Array, 1 October to 31 December, 1978, 25 pp.
30 December, 1979	Technical Report 1979-5: Seismic Event Log for Central Minnesota Seismic Array, 1 January to 31 March, 1979, 32 pp.
31 December, 1979	Quarterly Report.
1 March, 1980	Technical Report 1980-1: The East-Central Minnesota Earthquake of 14 May, 1979, 3 pp.
31 March, 1980	Technical Report 1980-2: Revised Epicentral Coordinates for Two Minnesota Earthquakes, 2 pp.
31 March, 1980	Accepted for publication in Bulletin of Seismological Society of America: Greenhalgh, S.A., H. M. Mooney, and C. C. Mosher: Some Results from the Central Minnesota Seismic Array.
31 March, 1980	Submitted for publication in Bulletin of Seismological Society of America: Mooney, H.M., and G. B. Morey: Seismic History of Minnesota and its Tectonic Significance.
31 March, 1980	Quarterly Report.
15 May, 1980	Ph.D. Thesis, University of Minnesota. Mosher, C.C., 1980, Signal Processing Techniques Applied to a Small Circular Seismic Array: xxii + 267 pp.

APPENDIX B: Oral Presentations at Meetings Based Upon Work Connected with Contract NRC-04-76-289

September, 1976 — Contractors meeting, U.S. Nuclear Regulatory Commission, Lawrence Kansas.

Harold M. Mooney

February, 1977 — Contractors meeting, U.S. Nuclear Regulatory Commission, St. Louis, Missouri.

Harold M. Mooney

June, 1978 — Eastern Network meeting, Golden Colorado.

Harold M. Mooney

September, 1978 — 2 papers presented: Midwestern Regional Meeting, American Geophysical Union, St. Louis, Missouri.

Stewart A. Greenhalgh

Greenhalgh, S.A., Mooney, H.M., and Mosher, C.C.: Magnitude calibration of the Central Minnesota Seismic Array.

Greenhalgh, S.A., and Mooney, H.M.: Seismic array studies of crustal structure in Minnesota.

May, 1979 — 1 paper presented: Annual Meeting, Seismological Society of America, Golden, Colorado.

Charles Mosher

Geological Interpretation of Travel Time and Magnitude Residuals on the Central Minnesota Seismic Array.

April, 1980 — 2 papers presented: Annual Meeting, Seismological Society of America, Seattle, Washington.

Charles Mosher

1. An Array Processing Technique for Azimuths and Phase Velocities of Surface Waves.
2. Epicenter Location without Travel Time Tables.

NRC FORM 335 (7-77) U.S. NUCLEAR REGULATORY COMMISSION

BIBLIOGRAPHIC DATA SHEET

1. REPORT NUMBER *(Assigned by DDC)*	NUREG/CR-1569
4. TITLE AND SUBTITLE *(Add Volume No., if appropriate)*	Seismicity and Tectonic Relationships for Upper Great Lakes Precambrian Shield Province
2. *(Leave blank)*	
3. RECIPIENT'S ACCESSION NO.	
7. AUTHOR(S)	Harold M. Mooney, Matt Walton
5. DATE REPORT COMPLETED	MONTH: June; YEAR: 1980
9. PERFORMING ORGANIZATION NAME AND MAILING ADDRESS *(Include Zip Code)*	Minnesota Geological Survey 1633 Eustis Street St. Paul, Minnesota 55108
DATE REPORT ISSUED	MONTH: July; YEAR: 1980
6. *(Leave blank)*	
8. *(Leave blank)*	
12. SPONSORING ORGANIZATION NAME AND MAILING ADDRESS *(Include Zip Code)*	Site Safety Research Branch Division of Reactor Safety Research Office of Nuclear Regulatory Research U.S. Nuclear Regulatory Commission Washington, D.C. 20555
10. PROJECT/TASK/WORK UNIT NO.	
11. CONTRACT NO.	FIN No. B5952
13. TYPE OF REPORT	Final technical report
PERIOD COVERED *(Inclusive dates)*	1976-1979
15. SUPPLEMENTARY NOTES	
14. *(Leave blank)*	

16. ABSTRACT *(200 words or less)*

This is a final report comprising a three year study of the seismicity of Minnesota including the procurement and installation of a six station seismograph system. This system was deployed in a microearthquake monitoring array. An earth model was developed based on signals from mine blasts and regular earthquake bulletins were published. Descriptions of the model, methodologies, and three significant earthquakes are given.

17. KEY WORDS AND DOCUMENT ANALYSIS	17a. DESCRIPTORS
17b. IDENTIFIERS/OPEN-ENDED TERMS	
18. AVAILABILITY STATEMENT	Unlimited
19. SECURITY CLASS *(This report)*	Unclassified
20. SECURITY CLASS *(This page)*	Unclassified
21. NO. OF PAGES	
22. PRICE	$

NRC FORM 335 (7-77)